We sincerely thank the Reviewer for their comments and insights. Please find our responses structured as follows:

- Original Reviewer comments in ***bold italics***
- Author responses as regular text
- Manuscript edits and changes in blue

Reviewer #1 Comments:

General remarks:

The authors present a new plume rise parameterization based on LES simulations using a synthetic plume-rise data set from WRF-SFIRE LES runs. The parameterization presented here is inexpensive and is able replicate fire plume rises that penetrate through the daytime PBL. Considering the current ongoing fires during the 2020 fire season, significant work is needed to better predict wildfire plume rises and smoke dispersion. As a result, the work carried out here is very timely and important.

With that said, the reviewer has some concerns in regard to the study presented here.

There are a number of plume rise modeling frameworks out there (Briggs, 1975; Sofeiv et al. 2012, Freitas et al. 2007; 2010), why develop yet another plume rise model? This should be made clear in the introduction section. For example, what is meant by an idealized heat source? Does this statement refer to the plume geometry?

The main goal of developing another plume-rise parameterization is that existing approaches remain subject to large uncertainties. For example, evaluation of BlueSky performance suggests that correlation coefficients associated with smoke injection predictions (based on adapted Brigg's algorithm) are on the order of 0.1 (Raffuse et al. 2012). Similarly low R^2-values (maximum of 0.33) were noted for Freitas model (Val Martin et al., 2012). Moreover, existing tools struggle to reliably differentiate which plumes remain in the ABL and which penetrate it (Val Martin 2012): information, which is key for subsequent dispersion modelling (Sofief et al. 2012). We added the following clarification at the end of the Introduction section:

…We then demonstrate with both numerical and prescribed burn data, that within the range of tested conditions this parameterization offers high speed and accuracy (Sect. 4). Moreover, it provides the means for classifying penetrative vs. non-penetrative plumes, which is key for subsequent dispersion modelling (Sofiev et al., 2012, Val Martin et al., 2012).

The proposed approach is geared toward regional smoke modelling frameworks (e.g. BlueSky and BlueSky Canada). Government agencies, air quality managers and fire response teams depend on these operational tools and their accuracy to issue air quality warnings, evacuation orders and to help mitigate human health impacts. Yet, model evaluation studies suggest that plume rise estimation remains a weak link within these smoke modelling systems (Raffuse et al., 2012, Val Martin et al. 2012, Chen et al. 2019). Moreover, existing methods struggle to reliably differentiate which plumes remain in the ABL and which penetrate. The broad goal of the work is, therefore, to address some of these challenges and improve the accuracy of plume rise predictions for regional air quality applications.

We added the following clarification regarding idealization of heat sources in Freita's and Rio's models:

…Notably, both consider an idealized heat source to represent the fire. To initialize the plume at the lower boundary, simplified fire geometry (circular and rectangular for Freita's and Rio's models, respectively) with a uniform heat flux is assumed.

The biggest limitation of this study is that it does not consider moisture sources, especially in the ambient atmosphere. Studies have shown that PyroCb development is strongly dependent on mid-level moisture. While PyroCbs are somewhat rare, these plumes are often responsible for some of the largest mass injections (2018) of smoke in the atmosphere, with some of these rivaling that of significant volcanic eruptions. PyroCus, which are far more common than PyroCb, are also strongly impacted by the vertical moisture profile (albeit less so then PyroCbs).

There are two important considerations regarding inclusion of moisture in the model (i) effects of ambient atmospheric moisture profile on plume development without saturation (ii) effects of latent heat release in plumes reaching condensation. Our proposed parameterization makes no assumptions regarding the former (e.g. the ambient sounding of the observational case study included moisture). The latter indeed remains to be addressed.

We certainly agree with the Reviewer that no-condensation assumption is the most significant limitation of the proposed model (as we explicitly state on Lines 270-274 of the original manuscript version). Apart from its accuracy, the reason we feel our parameterization is useful even in its current form is that vast majority of plumes are non-condensing. Based on remotely-sensed estimates, only 4-12% of the plumes over North America reach PBL top; amongst those that do, most (>83%) remain in the stable layers directly above PBL top (Val Martin 2010). While we are not aware of a formal climatology of pyroconvective events, analysis of a sample of remotely-sensed *high-altitude* plumes (above 5500m) over Yukon and Alaska suggests that less than 3% resulted in PyroCu formation (Val Martin 2010). This renders such events extremely rare.

Moreover, while formation of pyroconvective clouds undoubtedly effects *maximum* plume rise, it's effect on mean smoke injection height is less clear. Figure 1 below shows a plume height retrieval from MISR satellite (using MINX software) associated with Silver Fire in New Mexico in July 2013 (Nelson 2013). Notably, mean smoke injection height (subplot (c)) is largely unaffected by the presence of PyroCu.

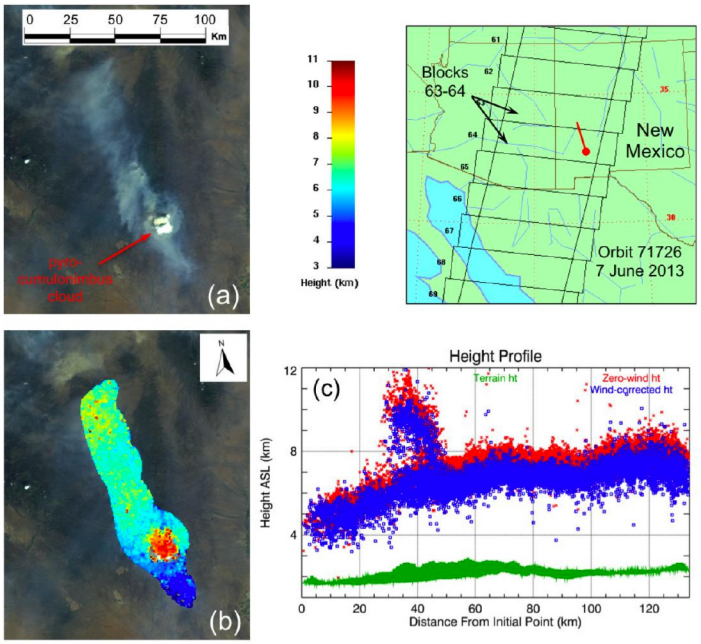

Figure 1. MINX plume height retrieval software output associated with the Silver Fire in New Mexico on MISR orbit 71726, block 63–64, from 12 July 2013 (Nelson 2013) (a) MISR nadir RGB image (b) MINX height retrievals (c) MINX height retrieval profiles

While inclusion of condensation is important for global chemical transport modelling application, regional smoke modelling frameworks (towards which this parameterization is geared) often do not consider moisture effects (e.g. BlueSky, BlueSky Canada, FireWork). That being said, we recognize the importance of extreme pyroconvective events, in particular for large scale applications. Detailed reasons for their exclusion from our current formulation as well as manuscript additions are addressed in comments below.

It was noted by the authors that weakly buoyant plumes that do not penetrate into the free troposphere were not considered as part of the data set. Why did the authors use the RxCADRE L2G as a case study? Overall, most of the RxCADRE prescribe burns were lower intensity fires. The largest burn (L2F), had a plume rise height that only reached an altitude of 1.5 km, which was still below the PBL. The reviewer does understand that there are a limited number of data sets where the plume rise is measured with constrained lower boundary conditions (i.e heat fluxes)

Apart from the uniquely comprehensive nature of the dataset, the reason we consider RxCADRE L2G is because it was indeed a penetrative plume (see response to Reviewer's "Specific Comments").

The reviewer has concerns that this study may be too limited in scope. The authors do not include plumes that fall below the PBL in their data set while this parameterization is only applicable for plumes that do not reach the lifting condensation level, which is height where plumes would be driven latent heat releases. As a result, it must be concluded that this parameterization will only valid for plumes greater than the PBL but less than the LCL, which seems like a narrow range of plumes that this parameterization is appropriate for. Furthermore, PyroCu and PyroCb events are usually associated with large fires that emit a lot of pollutants at high altitudes. Usually, its these smoke emissions that last the longest in the atmosphere (Peterson et al. 2018; Christian et al. 2019) and are the pollutants that fire researchers and forecasters are probably most interested in.

The presented parameterization is indeed valid for most (including PBL) plumes. We thank the Reviewer for pointing out that this was not made clear in the manuscript and hope that our additions address Reviewer's concerns.

While we did simulate boundary layer plumes (e.g. Figures 2 and 3 below), we excluded them from our training dataset because the concept of "injection height" is not relevant for non-penetrative cases. The smoke from such plumes becomes uniformly mixed throughout the depth of the turbulent PBL within several convective turnover periods. Often these low-buoyancy plumes initially exhibit irregular or oscillatory centerline behavior, rendering "injection height" concept irrelevant (see Figures 2 and 3 below). However, knowing which plumes will penetrate the PBL and which ones will not is critical for dispersion modelling (Val Martin et al. 2018, Sofiev et al. 2012). Our parameterization allows to determine this with encouraging accuracy. We, hence, revised our manuscript to include Section 5.1 and Appendix B, dedicated to LES simulations of non-penetrative and plume classification using our parameterization.

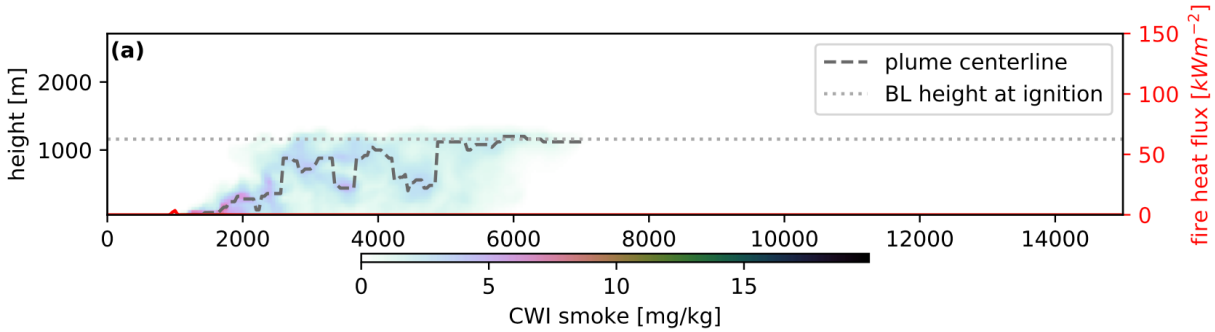

Figure 2. Oscillatory behavior of a sample non-penetrative plume in the boundary layer.

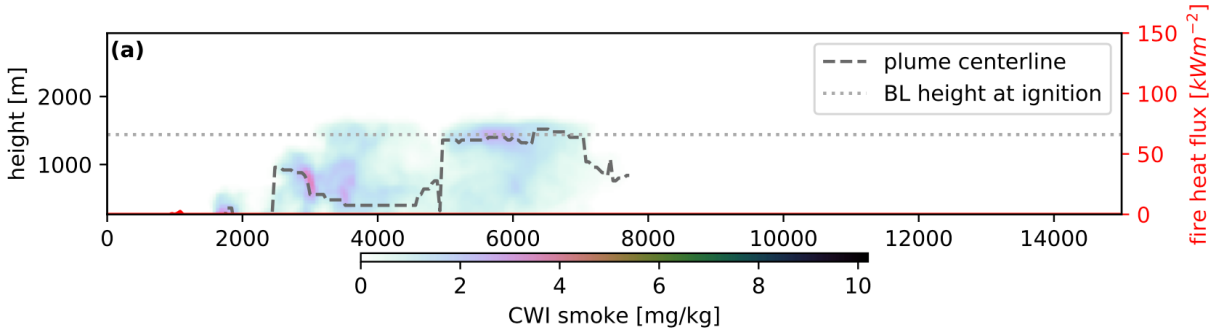

Figure 3. Irregular centerline behavior of a sample non-penetrative plume in the boundary layer.

Regarding condensation effects (PyroCu and PyroCb), we certainly acknowledge this as a limitation (see response to comment above). However, while our parameterized injection heights for such extreme events are likely to be underestimated, given typical prediction errors associated with existing models (on the order of kilometers) (Raffuse et al. 2012, Val Martin et al. 2012), they may well provide comparable performance.

Manuscript changes: Addition of Section 5.1 and Appendix B

As a result, the reviewer implores that the authors consider the effects of vertical moisture profiles within their parameterization. This work could be significantly more impactful if this limitation can be remedied as the parameterization presented here would have a clear advantage over the semi-empirical plume rise formulas discussed in Sofiev et al. (2012) and Briggs (1975).

As noted in our earlier response, our parameterization does not make assumptions about the vertical moisture profile for non-condensing plumes. We have explicitly considered ambient moisture in early model development stage. Figure 4 shows plume profiles under 'dry' and 'wet' (approximately 80% relative humidity, depending on the vertical level) environmental conditions, with the remaining parameters held constant. Note that the plumes are nearly identical, subject to random turbulence. The prediction error (obtained using iterative solution of our model) was 64 m for the 'dry' case and 14 m for the 'wet' case. Ambient moisture was also included in the evaluation case study (Section 4.3).

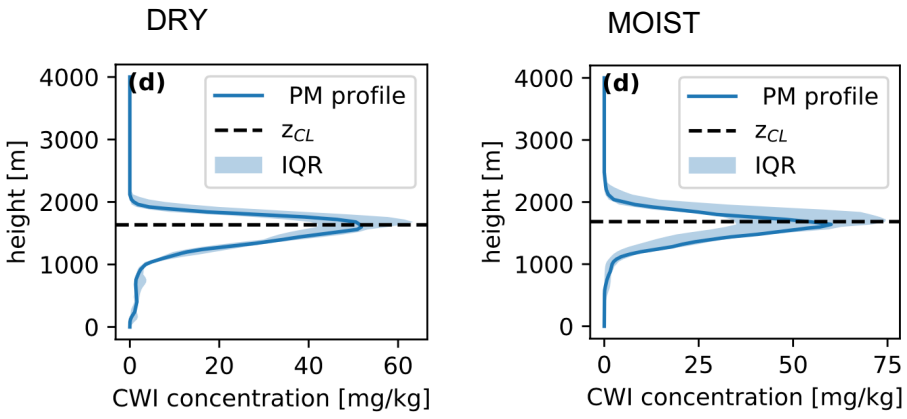

Figure 4. Plumes under 'dry' and 'wet' ambient atmospheric conditions (with remaining conditions held constant).

While we have confirmed that ambient moisture (without condensation) has little impact on our model performance, we agree with the Reviewer regarding the possible effects of PyCu. However, in order to include condensation and cloud formation, we first have to determine whether the LES can reasonably capture such conditions. To our knowledge, no such validation studies are available yet. Moreover, this modelling effort would require an evaluation dataset constraining not only the heat source and cloud development, but also the moisture fluxes parameterized by SFIRE. We hope that the current efforts of the FASMEE campaign (Prichard et al 2019) could make this possible in the near future. We added the following discussion to the Limitations section of the manuscript:

…The most significant limitation of the proposed smoke injection height parameterization is that it applies only to smoke plumes with no water vapor condensation. Latent heat effects are not considered. Hence, smoke injection level for extreme pyroconvective events (e.g. flammagenitus clouds (WMO 2017) will likely be grossly under-predicted with the given formulation. Therefore, in its current form, our parameterization is unlikely to be suitable for large-scale applications (e.g. global chemical transport models). However, it has the potential to improve regional air quality tools (e.g. BlueSky), since wildfire emissions sources are largely dominated by in- or near- ABL non-condensing smoke plumes (Val Martin et al., 2010, 2018).

Given the energy-balance formulation of our plume rise parameterization, it may be possible to incorporate latent heat effects by including an extra PE term in Eg. (1). Similarly to the iterative process for finding a level of neutral buoyancy with Eq. (8) using potential temperature, it may be possible to predict plume condensation level using ambient humidity profile. However, a big obstacle to this development is that, to our knowledge, WRF-SFIRE has not been validated for such conditions.

Specific comments:

Line 49: Mallia et al. 2018 did not use WRF-SFIRE, so this may not be an appropriate citation for this particular statement. Mallia et al. 2020 did use WRF-SFIRE though in their analysis though (see citation below).

Thank you for highlighting the error. We've changed the citation to Mallia et al. 2020.

Lines 52-58: While WRF-SFIRE is a well-documented coupled fire-atmosphere model, the authors should consider expanding the description for this modeling framework. Not all reviewers may be familiar with WRF-SFIRE.

We added the following short description to the manuscript at the beginning of Section 2:

…The model allows to explicitly resolve plume dynamics, while parameterizing fuel combustion. One of the primary advantages of using WRF-SFIRE is that it supports two-way coupling between the atmosphere and the fire behavior model, allowing it to capture some of the complex dynamical feedbacks that exist between the fire and the atmosphere (Prichard et al. 2019). Heat and moisture fluxes from the simulated burn provide forcing to the atmosphere, affecting local wind flow and thermodynamics. This in turn influences the modelled fire behavior.

Line 56: Why were these key parameters selected? For example, why not include ambient moisture? A number of well-known studies have shown that ambient moisture profile can significantly impact fire plume rise development, especially for PyroCb development (Freitas et al. 2007; Peterson et al. 2017; Tory et al. 2018)

Key parameter choices were largely dictated by what would be available as input from the host air quality model, as well as what has been broadly recognized as relevant in the literature. Our early simulations during model development also included various ambient surface heat fluxes (to examine the effect of ABL mixing) and moisture (see above). However, both of these factors did not appear to have a direct effect on our parameterization. We added the following clarification in the manuscript:

…Table 2 summarizes the key parameters that were varied to produce the synthetic dataset. The reason for considering the given conditions is twofold: these parameters (i) have been widely acknowledged as having a strong impact on plume behavior and (ii) can be obtained (and provided as input for the parameterization) under real-world scenarios.

Other manuscript changes (regarding condensation): Expanded Limitations section as per responses above.

Lines 53-78: A figure showing the numerical setup could be helpful to add here.

We added an illustration of the domain setup (and a corresponding in-text reference) as Appendix A.

Line 93-94: Can the authors provide recommendations on how atmospheric transport models should deal with weakly buoyant non-penetrative plumes that do not penetrate into the free troposphere?

Please see the response to a related comment above.

Manuscript changes: Addition of Section 5.1 on plume classification.

Lines 200-206: Why use RxCADRE when the authors were excluding plume rises that fell below the PBL height? Most of the RxCADRE burns were relatively small with plume rises that only reached an altitude of 1300 m.

As note in an earlier response, L2G burn indeed produced a penetrative plume. While the Reviewer is correct to note that the plume's maximum altitude may not be impressive, the boundary layer top during the burn was at roughly 1060 m (AGL). We added the following clarification in Section 4.3 of the manuscript:

…We use observational data from the RxCADRE L2G prescribed burn (Ottmar et al., 2016) and it's numerical simulation (Moisseeva and Stull, 2019). This case study was selected based on (i) comprehensive nature of the observational dataset (ii) penetration of the plume above ABL top and (iii) availability of a completed model validation study, confirming that WRF-SFIRE reasonably captures the smoke plume produced during the burn.

Lines 218-219: What time was the sounding relative to the start of the burn?

The pre-ignition sounding for L2G was performed at 10:00CST (i.e. 2h23min prior to the burn). We've added this in the manuscript:

…Due to wind shear, as measured by the sounding launched prior to the burn (10:00:00 CST), the CWI direction at the surface differs from the one used to estimate CWI smoke.

Lines 263: Is there a way that the author could test this hypothesis?

One way to examine whether additional mixing occurs above z_s is to consider conserved variable plots for plume centerlines. Figure 5 below compares plumes with shallow and deep penetration depths (note, the scales differ for both axes).

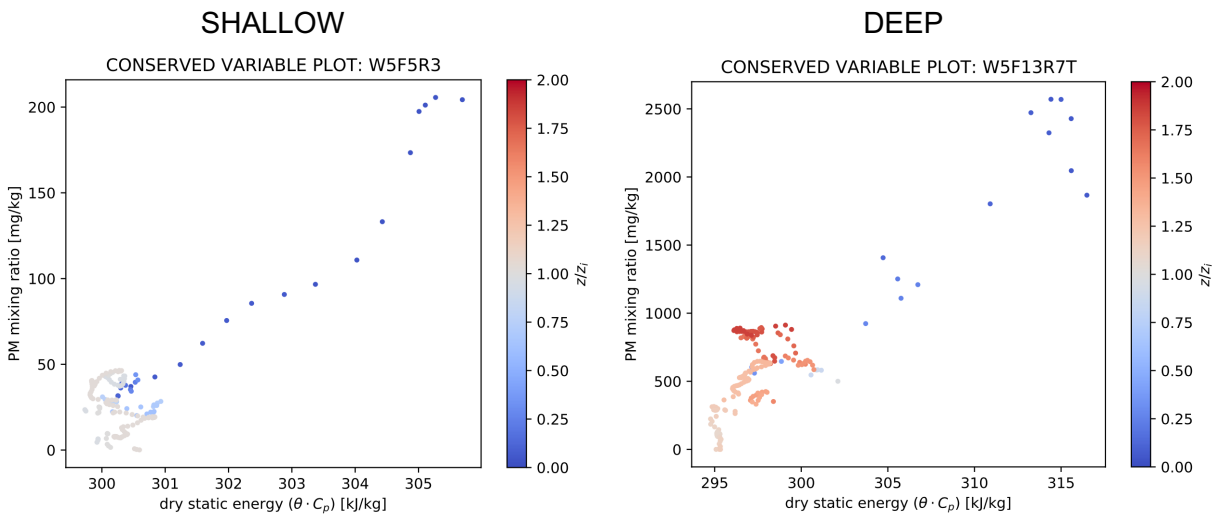

Figure 5. Conserved variable plots for shallow- and deep- penetrating plumes. Scatter point color correspond to normalized (by z_i) height of the centerline at the given location.

For the shallow case (left), little additional cooling occurs beyond boundary layer top (when the scatter points turn grey at $z/z_i=1$). For the deep case (right), there is a much more noticeable overshoot (deep red) of the centerline equilibrium height and obvious additional cooling occurring before z_{CL} is reached (light red). This generally supports our hypothesis. However, we do not see this occurring for all plumes. In part, this is expected, as the magnitude of the bias is on the order of general scatter in the data (see Figure 3 in the original manuscript). Hence, we do not feel we have sufficient evidence to draw conclusions.

Line 281: This conclusion section is really limited. Perhaps the authors could better synthesize the results in their study?

We edited the Conclusions section as follows:

Plume rise estimation remains one of the weakest links in our ability to forecast where and how smoke from wildfires travels in the atmosphere. In this study we present a simple parameterization (Eq. (8)) for predicting CWI smoke-plume centerline height from a wildfire of an arbitrary shape and intensity. Our approach is based on simple energy-balance of the plume over the penetration region. We constrain and evaluate the proposed method using a synthetic LES-derived plume dataset developed for a wide range of fire and atmospheric conditions.

Based on the results of cross-evaluation with LES data as well as a real prescribed burn case study, the parameterization offers reasonable accuracy at little computational cost. We demonstrate that the approach can also be applied as a classifier to distinguish penetrative and non-penetrative plumes. This information is key for subsequent dispersion modelling, as plume behavior is governed by different physics above and below the ABL. The proposed method can be used as a sand-alone deterministic model or embedded in a host smoke modelling framework.

We hope that parameterization presented in this study will be of interest to air-quality researchers to provide a low-cost solution for regional wildfire emissions-modelling applications.

In addition, this parameterization seems to be limited to plumes that fall above the PBL but less than the LCL (i.e cases where the is no PyroCu or PyroCb development). As a result, who is this parameterization geared towards? Why not just use the parameterization discussed in Freitas et al. 2007, which includes entrainment, wind shear (without restriction), and moisture effects. While the reviewer appreciates that this model can be run at a low computation cost, it seems like this parameterization comes with a number of cavaets that could limit its usefulness.

We hope our previous comments addressed model applications.

Manuscript changes: Addition of Section 5.1

This parameterization is geared towards regional air quality systems. Namely, it is most appropriate for smoke modelling frameworks, such as BlueSky and BlueSky Canada (which currently rely on adapted Briggs algorithms). We certainly agree that Freitas model is much better suited for global chemical transport modelling applications then our method.

Manuscript changes: Expanded Introduction section (see response to Reviewer's first general comment).

The overall reason for not using existing parameterisations is their somewhat discouraging performance (see response to Reviewer's first general comment). This can partly be partly attributed to uncertainties in fire input parameters - a source of error we don't have to worry about in LES simulations. However, parameterization of entrainment is actually a substantial limitation within prognostic models (including assumed instantaneous mixing along an idealized radially symmetric plume, constant empirical entrainment parameters, assumption of proportionality between vertical plume velocity and entrainment rate, among many others). These entrainment assumptions date back to tank experiments of Morton and Turner (Morton et al. 1956) for point buoyancy sources in uniformly stratified fluids, and it's questionable how applicable they are for wildfires. In part, explicit parameterization of windshear introduced in the later version of Freitas model aimed to remedy some of the limitations of the original entrainment assumptions (Freitas 2010). This is where LES can again offer a significant advantage, hence, its common use in other entrainment-focused fields, such as cloud physics (Dawe and Austin 2013).

Figure 1: This is not referenced in the text, except in the conclusion section.

The figure is referenced on line 90 (Section 2.2) of the original manuscript.

Figure 2a: Might be worthwhile to add distance to the x-axis here even though it is done in Figure 2b. Took a second to figure out what the x-axis was showing. The reviewer also recommends switching panels b and d since panel b corresponds to the plume in cross section (panel a)

We added the axes labels, as requested.

The main reason for the chosen subplot order is that the cross-section shown in panel (d) is based on the shaded quasi-stationary region identified in sublot (c). Therefore, we feel it's necessary to keep the order as is. We added a clarification in the caption:

…(d) Representative downwind smoke distribution. The profile (solid blue line) is obtained by horizontally averaging the CWI smoke concentrations in the quasi-stationary region (dashed grey in (c)).

References:

Dawe, J. T., and P. H. Austin. "Direct entrainment and detrainment rate distributions of individual shallow cumulus clouds in an LES." *Atmospheric Chemistry & Physics* 13.15 (2013).

Freitas, S. R., et al. "Sensitivity of 1-D smoke plume rise models to the inclusion of environmental wind drag." *Atmospheric Chemistry & Physics* 10.2 (2010).

Morton, B. R., Geoffrey Ingram Taylor, and John Stewart Turner. "Turbulent gravitational convection from maintained and instantaneous sources." *Proceedings of the Royal Society of London. Series A. Mathematical and Physical Sciences* 234.1196 (1956): 1-23.

Nelson, David L., et al. "Stereoscopic height and wind retrievals for aerosol plumes with the MISR INteractive eXplorer (MINX)." *Remote Sensing* 5.9 (2013): 4593-4628.

Raffuse, Sean M., et al. "An evaluation of modeled plume injection height with satellite-derived observed plume height." *Atmosphere* 3.1 (2012): 103-123.

Sofiev, M., T. Ermakova, and R. Vankevich. "Evaluation of the smoke-injection height from wild-land fires using remote-sensing data." *Atmospheric Chemistry & Physics* 12.4 (2012).

Val Martin, Maria, Ralph A. Kahn, and Mika G. Tosca. "A global analysis of wildfire smoke injection heights derived from space-based multi-angle imaging." *Remote Sensing* 10.10 (2018): 1609.

Val Martin, M., Logan, J. A., Kahn, R. A., Leung, F. Y., Nelson, D. L., & Diner, D. J. “Smoke injection heights from fires in North America: analysis of 5 years of satellite observations”. *Atmos. Chem. Phys*, *10*.4 (2010): 1491-1510.

We sincerely thank the Reviewer for their comments and insights. Please find our responses structured as follows:

- Original Reviewer comments in ***bold italics***
- Author responses as regular text
- Manuscript edits and changes in blue

Reviewer #2 Comments:

General remarks:

This paper introduces updraft velocity scales that are used during daytime CBLs. The scaling was developed using a set of model-derived synthetic plumes from WRF-SFIRE. The paper is novel and well-written. This reviewer feels that the observational dataset used is not ideal compared to other wildfire plume observations available. A limitation to the study and proposed methodology is the use of fireline intensity (heat flux) as this parameter is very difficult to observe in the field and even more so for wildfires. The data used are limited to the flame zone, but not the plume base. As the authors do recognize, the data from multiple sensors, have a range of values. It may be worthwhile to use sensible heat flux values calculated from the in situ tower observations. Overall, this is an excellent paper, well written and justified. I recommend publication after Minor Revisions.

We have explored using fire area and average heat flux instead of fireline intensity as input parameters for our model, however, we were not successful. We thank the Reviewer for pointing out this limitation. We added the following clarification in Section 5.5 (Limitations) of the manuscript:

Unlike many existing methods, our parameterization relies on fireline intensity parameter *I*, rather than average fire heat flux value, as input. While this approach offers an advantage for modelling plumes from complex ignition sources (such as shown in Fig. 8), fireline intensity is difficult to observe in the field.

We address observational datasets in the next comment.

While we are aware of the anemometer data from L2G in-situ tower, we find it's challenging to use as a means of quantifying fire behavior. Estimated sensible heat flux values naturally depend on the height from which the vertical velocity and temperature data are obtained, as well as the averaging period used. Also, given the variability amongst the in-fire sensors, we are hesitant to rely on observations from a single (tower) location.

While the proposed method for estimating plume rise is somewhat novel, it is unclear why the authors don't use more observational data. The authors state that observations are limited and that is somewhat true, but given the recent publication of key wildfire plume datasets (RaDFIRE; Clements et al. 2018), the authors should really use wildfire observations verses low-intensity prescribed fires from RxCADRE. Another issue with the methodology presented in this study is that the authors use a vertical velocity scale for plume rise, but have no vertical velocity observations. Vertical velocity data are also available from the RxCADRE dataset. Additionally, a very recent paper by Rodriguez et al. (2020) show deep updraft velocities in a megafire that could be used as an extreme boundary for the parameterization. Additionally, a dataset from Lareau and Clements (2017) of a wildfire that includes plume evolution in a cross-wind is available as was also used by (Mallia et al. 2019).

Key issue with both RaDFIRE dataset and the one described by Rodriguez et al. (2020), is that to our knowledge neither provides spatiotemporally linked fire behavior data. Lareau and Clements (2017) use inverted Brigg's equations to produce a rough estimate of fire heat flux. In the absence of fire behavior observations, it is not possible to properly constrain our model using these data.

While in-situ tower data from RxCADRE indeed include vertical velocities over the passing fire front, the observations are limited to near-surface heights. Our parameterized vertical velocity scale is calculated

over the plume penetration region starting from upper ABL. We feel that comparing it with near-surface data may not be meaningful.

We were unable to locate a reference matching Mallia et al. (2019). We did find a paper by Mallia et al. (2018), but they've considered RxCADRE L2F dataset in their study.

Some specific comments:

Line 148: It is not clear what the authors are defining as Fireline Intensity: ". . . fireline intensity parameter I, which is the kinematic heat flux into the atmosphere integrated across the fireline depth (in units of Km2s−1),. . ." I would call this the fire heat flux vs Byram's Fireline Intensity which has units of kW /m.

We've added the following clarification in the manuscript:
…This velocity scale is related to the fireline intensity parameter *I*, which is the kinematic heat flux into the atmosphere integrated across the fireline depth (in units of $Km^2\ s^{-1}$), and to the mixed-layer depth z_i. Note, that *I* effectively corresponds to the kinematic form of Byram's Fireline Intensity (in units of $kW\ m^{-1}$).

We maintained the kinematic form throughout the manuscript to ensure unit consistency in the model equations.

Line 205: Replace "lot" with "plot."

Corrected.

In Figure 2a, the mean plume centerline has a loop just downwind of the initial injection. Is this realistic? I would imagine that this feature represents the CBL, but would be averaged out as observed in the remainder of the downwind plume. Can the authors comment on this structure and whether this is realistic?

Figure 2a shows cross-wind integrated, rather than spatially/temporally averaged view of the plume. Hence, we would expect some random oscillatory centerline behavior near the heat source, driven not only by CBL thermals, but also fluctuations in fire intensity and propagation speed (at prior time steps). These fluctuations are naturally suppressed further downwind, as the plume settles in the stable layers above the CBL. Plume widening further masks these oscillations in cross-wind view. We added the following clarification to the manuscript (2nd paragraph of Section 2.3):

…As a result, our approach is based on defining a region, where the concentration distribution is quasi-stationary. We consider the last frame of each simulation for this analysis. Using CWI integrated tracer values, we locate the plume centerline (Fig. 2a). Due to random effects of ABL thermals as well as fluctuations in fire intensity and propagation speed, both centerline height and concentration can vary near the heat source. These oscillations are naturally suppressed in the stable layers above the ABL, as the plume travels downwind and undergoes additional widening and mixing.

References:

Lareau, Neil P., and Craig B. Clements. "The mean and turbulent properties of a wildfire convective plume." *Journal of Applied Meteorology and Climatology* 56.8 (2017): 2289-2299.

Mallia, Derek V., et al. "Optimizing smoke and plume rise modeling approaches at local scales." *Atmosphere* 9.5 (2018): 166.

Rodriguez, B., et al. "Extreme Pyroconvective Updrafts During a Megafire." *Geophysical Research Letters* 47.18 (2020): e2020GL089001.

Wildfire smoke-plume rise: a simple energy balance parameterization

Nadya Moisseeva[1] and Roland Stull[1]

[1]Department of Earth, Ocean and Atmospheric Sciences, The University of British Columbia, Vancouver BC V6T 1Z4, Canada

Correspondence: Nadya Moisseeva (nmoisseeva@eoas.ubc.ca)

Abstract. The buoyant rise and the resultant vertical distribution of wildfire smoke in the atmosphere have a strong influence on downwind pollutant concentrations at the surface. The amount of smoke injected vs. height is a key input into chemical transport models and smoke modelling frameworks. Due to scarcity of model evaluation data as well as inherent complexity of wildfire plume dynamics, smoke injection height predictions have large uncertainties. In this work we use a coupled fire-atmosphere model WRF-SFIRE configured in large eddy simulation (LES) mode to develop a synthetic plume dataset. Using this numerical data, we demonstrate that crosswind integrated smoke injection height for a fire of arbitrary shape and intensity can be modelled with a simple energy balance. We introduce two forms of updraft velocity scales that exhibit a linear dimensionless relationship with the plume vertical penetration distance through daytime convective boundary layers. Lastly, we use LES and prescribed burn data to constrain and evaluate the model. Our results suggest that the proposed simple parameterization of mean plume rise as a function of vertical velocity scale offers reasonable accuracy (30 m errors) at little computational cost.

1 Introduction

Predictions of surface concentrations of wildfire smoke by regional and global chemical transport models depends on the initial equilibrium height of the smoke plume. Plume rise, which determines this equilibrium height, is widely recognized as an area of uncertainty (Goodrick et al., 2013; Paugam et al., 2016). Traditionally, many operational smoke modelling frameworks relied on plume rise equations originally developed by Briggs (1975) for industrial smokestacks (Larkin et al., 2010; Pavlovic et al., 2016). Yet several studies suggest that this approach may not be appropriate for wildfires (Pavlovic et al., 2016; Heilman et al., 2014; Freitas et al., 2007).

In a recent review of existing plume rise parameterizations, Paugam et al. (2016) highlight three notable models that stand out in literature, as that of Freitas et al. (2007), Sofiev et al. (2012) and Rio et al. (2010). Both Freitas and Rio's approaches use first principles to characterize plume temperature, vertical velocity and entrainment. While the former provides prognostic 1-D equations that can be solved as a stand-alone "offline" model, the latter is implemented as a sub-grid effect within a host chemistry transport model. Notably, both consider an idealized heat source to represent the fire. To initialize the plume at the lower boundary, simplified fire geometry (circular and rectangular for Freita's and Rio's models, respectively) with a

uniform heat flux is assumed. Sofiev's semi-empirical approach relies on energy balance and dimensional analysis, while using satellite data to both initialize and constrain the parameterization. Unlike Briggs's equations, all of the above models address wildfire plumes specifically, yet much research is needed to reduce the large uncertainties associated with the model predictions (Mallia et al., 2018). Moreover, it is unclear, whether unreliable predictions should be attributed to the fire input parameters or the plume rise model itself.

One of the central challenges in plume rise model development has been the scarcity of comprehensive model evaluation data (Coen et al., 2012b; Ottmar et al., 2016). To date, information on wildfire smoke emissions and dispersion has largely been derived from two distinct sources: remotely sensed data and prescribed burn campaigns. While increasing numbers of satellite observations contribute to a more complete plume climatology (Val Martin et al., 2010), the data is subject to biases and lacks direct spatiotemporal links to fire behavior (Ichoku et al., 2012). In contrast, field campaigns, such as Prescribed Fire Combustion and Atmospheric Dynamics Research Experiment (RxCADRE) (Ottmar et al., 2016) and Fire and Smoke Model Evaluation Experiment (FASMEE) (Prichard et al., 2019), provide the necessary level of detail for model validation studies. However, such datasets typically capture a modest range of fire and atmospheric conditions.

Our approach, therefore, is to develop a synthetic plume dataset that addresses the limitations of the available observational data. As vast majority of smoke plumes remain in or just above the atmospheric boundary layer (ABL) (Val Martin et al., 2010; Mallia et al., 2018), we use large eddy simulations (LES) to focus on local- and meso- scale plume dynamics. Using a coupled model, we simulate a wide range of fire and atmospheric conditions (Sect. 2). Based on this synthetic LES data (hereafter referred to as "data") we propose a simple energy balance model for predicting plume rise of crosswind integrated (CWI) smoke from a non-uniform fireline (Sect. 3). We use the synthetic plume dataset to constrain and evaluate our plume rise parameterization. We then demonstrate with both numerical and prescribed burn data, that within the range of tested conditions this parameterization offers high speed and accuracy (Sect. 4). ~~Our hope is that the proposed smoke plume rise parameterization will help improve smoke dispersion predictions within air quality applications. The ultimate goal is to provide better health and evacuation warnings to communities downwind of wildfires~~Moreover, it provides the means for classifying penetrative vs. non-penetrative plumes, which is key for subsequent dispersion modelling (Sofiev et al., 2012; Val Martin et al., 2012).

The proposed approach is geared toward regional smoke modelling frameworks (e.g. BlueSky and BlueSky Canada). Government agencies, air quality managers and fire response teams depend on these operational tools and their accuracy to issue air quality warnings, evacuation orders and to help mitigate human health impacts. Yet, model evaluation studies suggest that plume rise estimation remains a weak link within smoke modelling systems (Raffuse et al., 2012; Val Martin et al., 2012; Chen et al., 2019). Moreover, existing methods struggle to reliably differentiate which plumes remain in the ABL and which penetrate it. The broad goal of the work is, therefore, to address some of these challenges and improve the accuracy of plume rise predictions for regional air quality applications.

2 Development of a Synthetic Plume Dataset

We devise a synthetic plume data set using a coupled fire-atmosphere model WRF-SFIRE, which combines the well-established Weather and Research Forecasting Model (WRF) with a semi-emperical fire spread algorithm called SFIRE ~~(Mandel et al., 2014; Mallia et a~~ ~~. The~~ (Mandel et al., 2014; Mallia et al., 2020; Coen et al., 2012a; Kochanski et al., 2013; Clements et al., 2006; Kochanski et al., 2019) . The model allows one to explicitly resolve plume dynamics, while parameterizing fuel combustion. One of the primary advantages of using WRF-SFIRE is that it supports two-way coupling between the atmosphere and the fire behavior model, allowing it to capture some of the complex dynamical feedbacks that exist between the fire and the atmosphere (Prichard et al., 2019) . Heat and moisture fluxes from the simulated burn provide forcing to the atmosphere, affecting local wind flow and thermodynamics. This in turn influences the modelled fire behavior. The following sections detail the numerical setup of WRF-SFIRE, scope of the dataset, as well as our approach to defining "ground truth" for model evaluation.

2.1 Numerical Configuration

WRF-SFIRE was configured in idealized large-eddy resolving mode. Much of our numerical setup was adopted from a case study of a real prescribed burn as detailed in Moisseeva and Stull (2019), to ensure the simulations represent physical conditions backed by model evaluation. Due to high computational demands of LES runs, we focused on the local- and meso- scales, considering only the initial buoyant plume rise of smoke in typical daytime atmospheres. Key parameters varied were ambient wind, fuel category, vertical potential temperature profile and fireline length, denoted as conditions **W**,**F**,**R** and **L**, respectively (detailed further in Sect. 2.2).

Each 10 km x 20 km domain with 40 m horizontal grid spacing was initialized with uniform ambient west wind **W** and vertical temperature profile **R**. Depending on the sounding **R**, the simulations were performed in either a shallow (3000 m) or a deep (5000 m) domain, with 51 or 71 hyperbolically stretched vertical levels, respectively. A constant uniform lower boundary surface thermal flux (tke_heat_flux) in the ambient environment and lateral periodic boundary conditions were imposed to produce a turbulent well-mixed layer. We used full surface initialization (sfc_full_init =.true.), with the lower boundary characteristics set to USGS values for land use most closely matching the Anderson fuel category **F** (Anderson, 1982). The corresponding surface roughness lengths added various levels of wind shear to each domain to produce a more realistic non-uniform vertical wind profile during spinup of the environment before the fire was initialized in the LES.

Initial convection in the ambient environment was triggered using a perturbed surface temperature field. On average, a near-stationary turbulence spectrum was achieved within the first 30 min of run start. The "restart" file generated at the end of one hour of spinup was used to initialize the main burn simulation, ensuring the fire was ignited in a well-mixed turbulent ABL.

The fire was initialized over a one-minute interval using a straight line of length **L**. The ignition line was placed one kilometer downwind of the western edge of the domain and centered in the north-south direction (sample illustration of this setup can be found in Appendix A). With a refinement ratio of 10 in each horizontal direction, the fire was simulated on a 4 m sub-grid mesh.

Table 1. Key parameters of numerical domain setup.

Simulation Parameter	Value/Description
Model version	May 24, 2019 (git #ced5955)
Horizontal grid spacing	40 m
Domain size	500 grids cells (east-west) x 250 grids cells (north-south)
Time step	0.1 s
Model top	3000 m (shallow) / 5000 m (deep)
Spinup timing	11:30:00 - 12:30:00
Fire (restart) simulation timing	12:30:00 - 12:50:00 (shallow) / 12:30:00 - 13:00:00 (deep)
Sub-grid scale closure	1.5 TKE (TKE = Turbulence kinetic energy)
Lateral boundary conditions	periodic
Surface physics	Monin-Obukhov similarity (sf_sfclay_physics = 1)
Land surface model	thermal diffusion (sf_surface_physics = 1)
Ambient surface heat flux	240 Wm^{-2}(tke_heat_flux=0.2)
Fire mesh refinement	10
Ignition duration	13:00:10 – 13:01:10
Heat of combustion of dry fuel	16.4e+06 J kg^{-1}

The "smoke plume" was modelled with a passive tracer emitted proportionally to the mass and type of fuel burned. The rate of release was controlled by an assigned emission factor representing $PM_{2.5}$ for each fuel category, based on values provided by Prichard et al. (2017) (see namelist.fire_emissions in Supplementary Material).

A summary of key configuration details can be found in Table 1, as well as in sample namelist initialization files provided as Supplementary Material.

2.2 Test Conditions

Table 2 summarizes the key parameters that were varied to produce the synthetic dataset. The reason for considering the given conditions is twofold: these parameters (i) have been widely acknowledged as having a strong impact on plume behavior and (ii) can be obtained (and provided as input for the parameterization) under real-world scenarios.

The range of ambient winds tested was bound largely by numerical constraints. Due to cyclic boundary conditions, wind speeds higher than 12 ms^{-1} would require a much larger domain to prevent smoke recirculation. For the lower bound on our wind condition **W**, we needed to ensure that sufficient wind speed was maintained to propagate the fire. The spread algorithm used within the LES applies a correction factor under low wind speed conditions to prevent the fire from extinguishing itself. While necessary for numerical reasons this effect is not physical, so winds below 3 ms^{-1} were excluded from our dataset.

We used 9 different atmospheric profiles (**R** condition) to initialize the model. We varied the following features for each initialization:

Table 2. Test conditions included in synthetic plume dataset. The count indicates the number of unique values used within the specified range.

Condition (Tag)	Range	Count	Description
Ambient wind (W)	3 - 12 ms^{-1}	10	Uniform horizontal wind magnitude used to initialize model spinup
Stability profile (R)	R0-R8	9	Atmospheric sounding with variable ABL height, temperature and inversion strength
Fuel (F)	1 - 13	13	Anderson fuel category assigned at lower boundary
Fireline length (L)	1 - 4 km	3	Length of ignition line
			Total number of experiments = 140

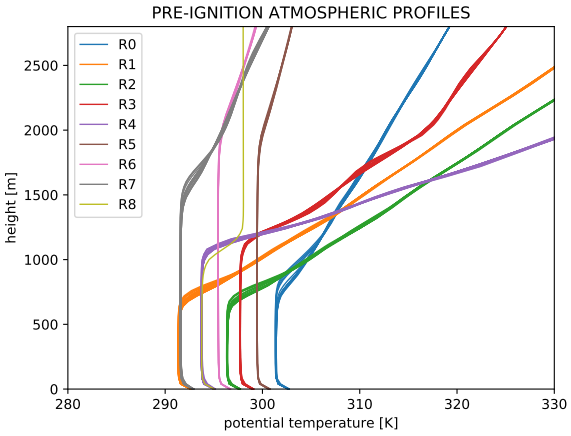

Figure 1. Pre-ignition potential temperature profiles (stability condition **R**). Colors correspond to initial soundings used for model spinup.

- initial ABL height (500 m - 1600 m)
- potential temperature lapse rate above inversion (0 $\mathrm{K\ km}^{-1}$ - 20 $\mathrm{K\ km}^{-1}$)
- initial ABL temperature (290 K - 300 K)

Following spinup (Sect. 2.1) under variable winds and surface conditions, this produced 9 sets of soundings, shown in Fig. 1 with ABL depths of approximately 600 m - 2000 m.

We tested all fuel categories available within the model (**F** condition), and varied the length of the fireline (**L** condition) between 1 and 4 km. Weakly buoyant non-penetrative plumes whose smoke remained within the well-mixed ABL were excluded from the dataset, as their behavior is governed by different physics. A tabulated summary of all combinations included can be found in Appendix B.

Note, that varying a single condition while holding the rest constant does not result in a controlled experiment isolating its impact on plume rise. Because WRF-SFIRE incorporates fire-atmosphere coupling, the problem is not well-constrained. For example, by varying fuel type **F** alone, while holding the rest of test conditions constant, we obtain a set of fires with diverse shapes, sizes, intensities, fireline depths, rates of spread and heat release. This reflects the complexity of non-linear interactions that exist between the fire and the atmosphere. As a result, the parameter space captured within our LES dataset is much greater then the four conditions described in Table 2.

2.3 Defining Smoke Injection Height

Given non-stationary fire and atmospheric conditions, determining a consistent definition of an equilibrium smoke injection height is not a trivial task. It requires separating buoyant rise from dispersion, while excluding the effects of initial momentum overshoot and accounting for the advection due to varying ambient and fire-generated winds.

A common way of examining vertical distributions of pollutants in the context of air quality is to consider CWI concentrations. This allows to reduce the problem to two dimensions, with plume centerline being defined simply as the CWI concentration maximum at each location downwind of the source. Theoretically, under stationary conditions there exists an equilibrium height, around which the centerline eventually oscillates. In reality, as well as in our LES experiments, neither the ambient nor the fire conditions are stationary. The changing location, shape and intensity of the fire, ABL warming and growth, as well as the development of fire-coupled winds and vorticity continually modify the conditions.

As a result, our approach is based on defining a region, where the concentration distribution is quasi-stationary. We consider the last frame of each simulation for this analysis. Using CWI integrated tracer values, we locate the plume centerline (Fig. 2a). Due to random effects of ABL thermals as well as fluctuations in fire intensity and propagation speed, both centerline height and concentration can vary near the heat source. These oscillations are naturally suppressed in the stable layers above the ABL, as the plume travels downwind and undergoes additional widening and mixing. To obtain the quasi-stationary region for each individual plume, we first calculate the change in tracer concentration along the centerline. We then use a smoothing function to reduce the effect of random turbulent oscillations in both the centerline height and the tracer concentration gradient along the centerline. The downwind region where both of these parameters are not changing rapidly are then then considered quasi-stationary. Additional details of this filtering method are provided in Appendix C.

The vertical CWI distribution of tracers are then averaged in the downwind direction over the identified quasi-stationary regions (shaded in grey on the Fig. 2c) to produce a representative downwind distribution for each plume (Fig. 2d). We define the "true" injection height z_{CL} as the mean height of smoothed centerline over the averaging region. The resultant dataset of z_{CL} values is used to constrain and evaluate the proposed smoke injection height parameterization introduced in the following sections.

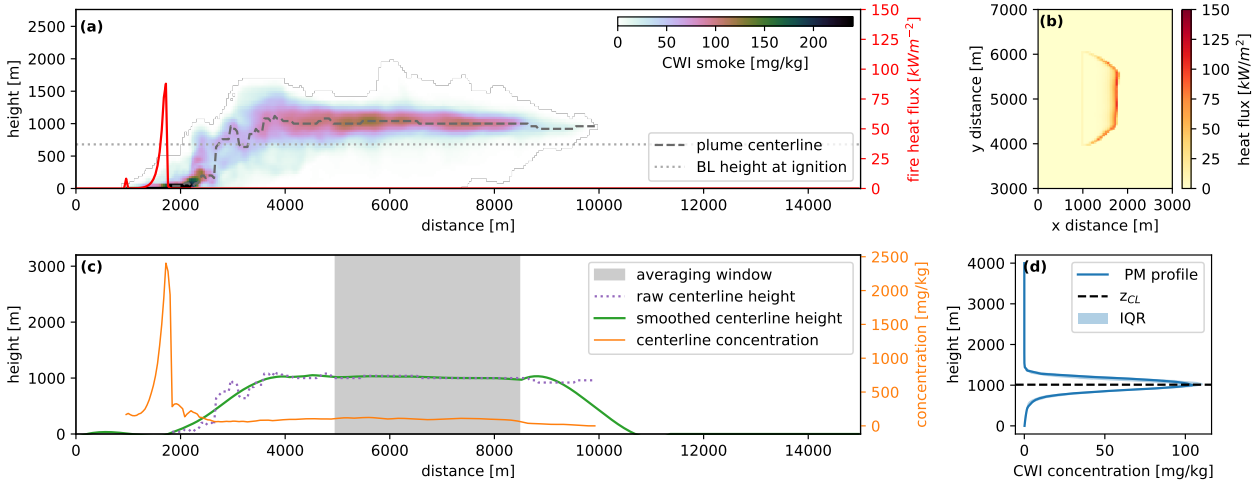

~~Illustration of the approach to identifying a quasi-stationary downwind region in CWI smoke distribution using a sample LES experiment. (a) CWI smoke concentrations. Also shown are plume centerline height (dashed), z_i (dotted) and CWI fireline intensity (solid red, secondary axis). (b) Plan view of fire heat flux showing the fireline. (c) Quasi-stationary region (grey shading). Also shown are raw (dotted purple) and smoothed (solid green) centerline heights and the tracer concentration gradient (solid orange, secondary axis). (d) Representative downwind smoke distribution. The profile (solid blue line) is obtained by horizontally averaging the CWI smoke concentrations in the quasi-stationary region. Also shown are IQR (light blue shading) and the derived smoke injection centerline height z_{CL} (dashed black).~~

Figure 2. Illustration of the approach to identifying a quasi-stationary downwind region in CWI smoke distribution using a sample LES experiment. (**a**) CWI smoke concentrations. Also shown are plume centerline height (dashed), z_i (dotted) and CWI fireline intensity (solid red, secondary axis). (**b**) Plan view of fire heat flux showing the fireline. (**c**) Quasi-stationary region (grey shading). Also shown are raw (dotted purple) and smoothed (solid green) centerline heights and the tracer concentration gradient (solid orange, secondary axis). (**d**) Representative downwind smoke distribution. The profile (solid blue line) is obtained by horizontally averaging the CWI smoke concentrations in the quasi-stationary region (dashed grey in (c)). Also shown are IQR (light blue shading) and the derived smoke injection centerline height z_{CL} (dashed black).

3 Smoke Injection Height Model for Penetrative Wildfire Plumes

A common approach to predicting the final equilibrium centerline height of wildfire smoke is to first estimate the initial buoyant energy of the hot rising smoke (Briggs, 1975; Sofiev et al., 2012; Anderson et al., 2011). After the smoke plume entrains surrounding ABL environmental air and cools, the remaining energy is spent doing work to push the cooled smoke plume up into the statically stable capping inversion.

The relationship between final and initial energies is often rewritten to show that the potential energy per unit mass (PE) of smoke penetration equals some fraction c_1 of initial heat released from the fire. In kinematic units, the initial heat input has

units similar to a kinetic energy per unit mass (KE). The empirical parameter c_1 is usually estimated based on concepts of entrainment into the rising smoke plume (Cushman-Roisin, 2014).

$$PE = c_1 KE \tag{1}$$

The PE of smoke-plume penetration into the capping inversion can be written as

$$PE = g' z' \tag{2}$$

where the penetration distance z' of the final equilibrium smoke centerline z_{CL} above reference height z_s (near the top of the well-mixed portion of ABL) is

$$z' = z_{CL} - z_s \tag{3}$$

The static-stability variable g' for the plume-penetration region is

$$g' = g\frac{\theta_{CL} - \theta_s}{\theta_s} = g\frac{\theta'}{\theta_s} \tag{4}$$

where θ_{CL} and θ_s are the potential temperatures of the ambient environment at z_{CL} and z_s, respectively, and $\theta_{CL} - \theta_s = \theta'$.

The KE can be estimated using a velocity scale w_f as

$$KE = 0.5 w_f^2 \tag{5}$$

Traditionally, the bulk potential-temperature difference across the smoke-plume penetration region θ' is expected to be relevant for only the PE portion of Eq. (1). However, we found from the LES runs for a wide range of fire and environment conditions that the KE also depends on the same potential temperature difference. This dependence can be expressed in the velocity scale:

$$w_f = \frac{I}{z_i \theta'} \tag{6}$$

This velocity scale is related to the fireline intensity parameter I, which is the kinematic heat flux into the atmosphere integrated across the fireline depth (in units of $\mathrm{Km^2 s^{-1}}$), and to the mixed-layer depth z_i. Note, that I effectively corresponds to the kinematic form of Byram's Fireline Intensity (in units of $\mathrm{kWm^{-1}}$).

We speculate that this interesting result is because smoke from a fire does not rise through a passive environment, as is often assumed for Briggs types of plume entrainment models. Instead, the fire and the environment interact in many complex ways. Some of these include: vertical-to-bent-over vortices on the ends of the fire line that rapidly mix environmental air into the buoyant smoke plume; modulation of fire intensity and fire updrafts by translation of ambient thermals across the fire line; plumes of enhanced convergence and updraft along the fire line; mass conservation as descending air beneath the extended smoke plume lowers the local mixed-layer depth; and other factors.

Thus, Eq. (1) becomes

$$g' z' = c_2 \left[\frac{I}{z_i \theta'}\right]^2 \tag{7}$$

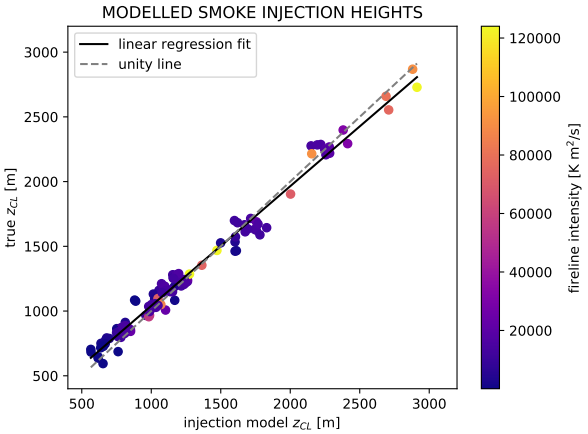

Figure 3. Comparison of true (as shown in Fig. 2) and modelled (from Eq. (8)) smoke injection heights. Scatter points represent the 140 individual plume experiments within the LES dataset, with colors corresponding to fireline intensity I. Solid black and grey dashed lines denote linear regression fit and unity, respectively.

where $c_2 = 0.5c_1$.

The above can be rearranged into the following form

$$z_{CL} - z_s = C\left[\frac{g\left(\theta_{CL} - \theta_s\right)}{\theta_s\left(z_{CL} - z_s\right)}\right]^{-\frac{1}{2}}\left\{\frac{gI\left(z_{CL} - z_s\right)}{\theta_s z_i}\right\}^{\frac{1}{3}} \tag{8}$$

where the dimensionless empirical parameter is $C \approx 1$. The factors in square and curly brackets with their corresponding powers have units of time and velocity, respectively. This relationship is plotted in Fig. 3. It provides quite an acceptable fit to the data over a wide range of 140 combinations of fire and atmospheric conditions simulated.

Equation (8) suggests that the relevant length and temperature scales (z', θ') depend not on the capping inversion strength alone, or on the tropospheric lapse rate above the capping inversion alone, but on the bulk potential-temperature differences across the smoke-plume penetration region, $z_{CL} - z_s$. Eq. (8) is implicit, in that the desired plume centerline equilibrium height z_{CL} appears in both the left and right sides of the equation. The plume centerline height also defines where θ_{CL} is retrieved from the atmospheric sounding; namely, z_{CL} is implicit in both Eq. (7) and (8). However, for any specific fire and environment conditions, values of z_{CL} are easily found by iteration (see Appendix E). Steps to estimating input parameters required for the proposed injection model from the LES data are summarized in Appendix D.

Alternatively, for a small sacrifice in accuracy, we can obtain an explicit solution by considering an idealized version of the atmospheric profile, consisting of an adiabatic mixed layer, entrainment zone and a stable uniformly stratified free atmosphere above (Fig. 4). In such case γ is defined as the overall potential temperature gradient of the free atmosphere and z_s as the height corresponding to the intercept of γ and the well mixed portion of the ABL profile. Then, using Eq. (8), z_{CL} can be

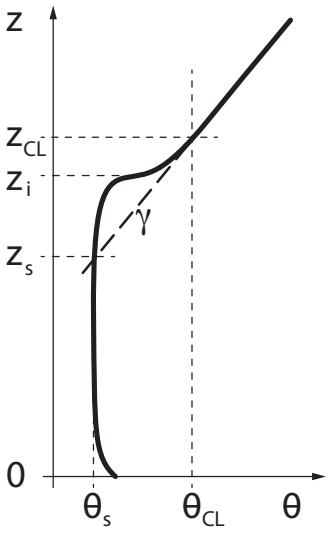

Figure 4. Idealized potential temperature profile θ vs. height with constant stable layer lapse rate γ.

found explicitly as:

$$z_{CL} = C^{\frac{3}{2}} \left[\frac{\theta_s}{g}\right]^{\frac{1}{4}} \left[\frac{I}{z_i}\right]^{\frac{1}{2}} \left[\frac{1}{\gamma}\right]^{\frac{3}{4}} + z_s \tag{9}$$

4 Results

To assess the accuracy of the proposed smoke injection height parameterization (Eq. (8)), we performed two sets of verification studies. The first approach is based on using the synthetic plume dataset to perform model evaluation, bias correction and sensitivity analysis with idealized data. The second portion of this section applies our approach to a case study of a real prescribed burn (RxCADRE 2012).

4.1 Numerical Results

Shown in Fig. 3 are "true" and parameterized smoke injection heights. The former is obtained directly from the LES, as per Sect. 2.3. The latter is determined iteratively using the proposed smoke injection height parameterization (see Appendix E for implementation details).

Individual prediction errors do not appear to be a function fireline intensity, as indicated by scatter point color in Fig. 3, or ambient winds (not shown). While overall the model performance is encouraging, the small discrepancy between the unity and regression lines suggests a linear bias. This can be remedied by applying bias correction using regression parameters from the

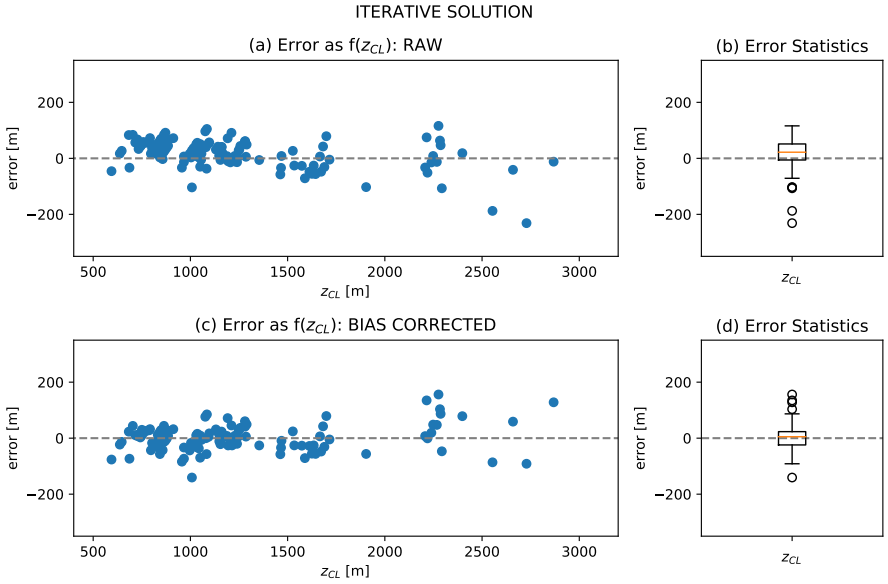

Figure 5. Performance of the smoke injection height parameterization based on the iterative solution (Eq. (8)). (a) Non-bias corrected model prediction error (true - modelled z_{CL}) as a function of z_{CL}. (b) Error statistics for non-bias corrected model. The box and whiskers span interquartile range (IQR) and 1.5 x IQR, respectively. Median value shown in orange. (c) Bias-corrected model prediction error as a function of z_{CL}. (d) Error statistics for bias-corrected model.

fit shown in Fig. 3. This optimized model produces errors on the order of 20 - 30 m, as suggested by the interquartile range shown in Fig. 5d. Model bias will be addressed in further detail in Sect. 5.

Given smooth averaged profiles from the synthetic dataset and excluding condition **R8** (adiabatic free atmosphere), the explicit solution using Eq. (9) offers comparable accuracy to the iterative version for both raw and bias corrected datasets (Fig. 6) . We address the limitations of using the explicit approach in Sect. 5.5.

4.2 Model Sensitivity

To asses how sensitive the smoke injection model performance is to the particular choice of bias correction parameters, we partition our original plume dataset into training and testing groups through random sampling. We obtain the linear bias correction parameters using training data only (80% of runs). We then apply our bias-corrected iterative solution to the test group (remaining 20% of the runs) and assess model accuracy. Figure 7 summarizes model performance and sensitivity, based on 10 trials of sampling with replacement. Consistently high Pearson correlation shown in the trial histogram in Fig. 7c, are encouraging, and suggest that the particular choice of simulations used in bias correction does not have a strong impact on model accuracy.

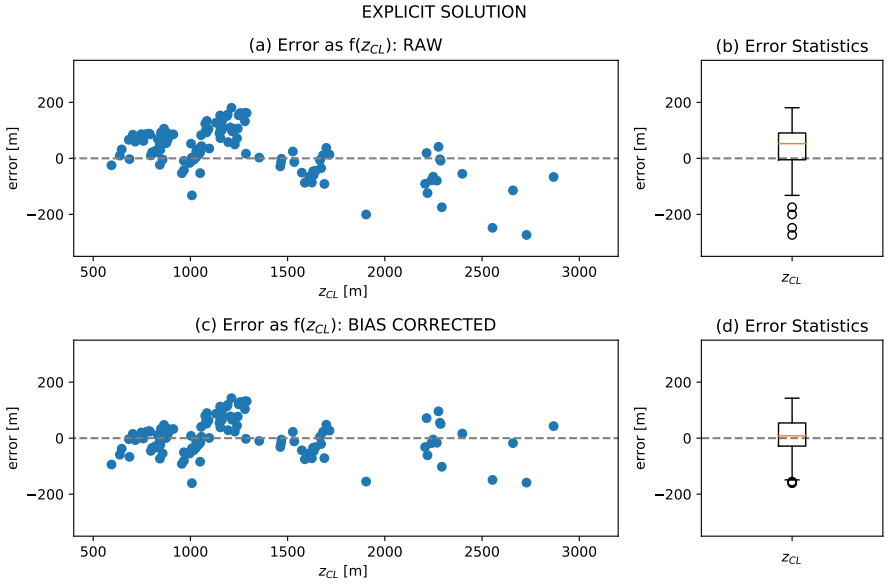

Figure 6. Performance of the smoke injection height parameterization based on the explicit solution (Eq. (9)). (a) Non-bias corrected model prediction error (true - modelled z_{CL}) as a function of z_{CL}. (b) Error statistics for non-bias corrected model. The box and whiskers span interquartile range (IQR) and 1.5 x IQR, respectively. Median value shown in orange. (c) Bias-corrected model prediction error as a function of z_{CL}. (d) Error statistics for bias-corrected model.

4.3 Evaluation with Observations

Next, we apply the proposed model to a real-life case-study. We use observational data from the RxCADRE L2G prescribed burn (Ottmar et al., 2016) and it's numerical simulation (Moisseeva and Stull, 2019). This case study was selected based on (i) comprehensive nature of the observational dataset (ii) penetration of the plume above ABL top and (iii) availability of a completed model validation study, confirming that WRF-SFIRE reasonably captures the smoke plume produced during the burn.

Shown in Fig. 8 is the strip headfire pattern used to ignite the grass ~~lot~~plot. We estimate the burn's input fireline intensity parameter I in two different ways: from raw data collected during the burn as well as from the numerical simulation.

The observations-based value I_{obs} is derived from the integral heat flux data obtained from the Highly Instrumented Plots (HIPs) fire behavior package (FBP) sensors (Jimenez and Butler, 2016). We use the provided time-integrated values, averaging between all sensors with confirmed fire at the sensor location (as indicated by video footage (Butler et al., 2016)). We then obtain the mean value (in kinematic units) of 236 Kms^{-2} and multiply it by the average measured rate of spread (ROS) of 0.38 ms^{-1} (Butler et al., 2016) for the same sensors to convert to spatially-integrated heat flux for a single fire line. We assume that this value is representative of the remaining three firelines, hence:

$$I_{obs} = 236 \cdot 0.38 \cdot 4 = 359 \tag{10}$$

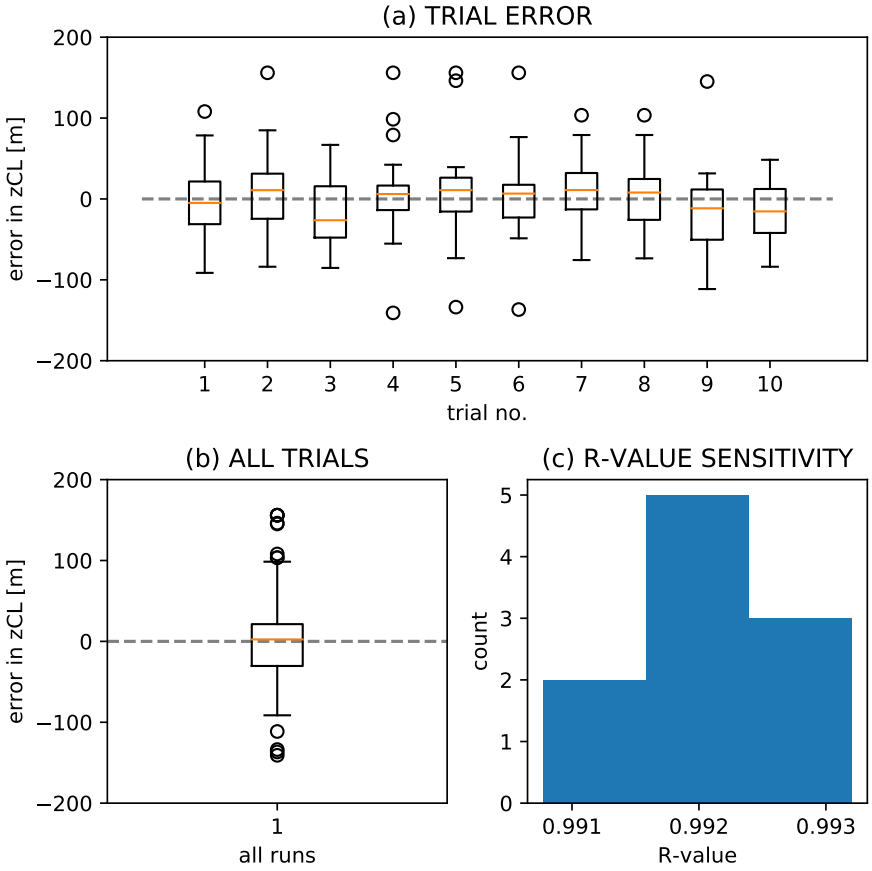

Figure 7. Analysis of model sensitivity to the choice of bias correction parameters. (a) Error distributions for individual trials using independent (test) data. (b) Error distribution for all trials using independent (test) data. (c) Sensitivity of R-value (correlation coefficient) for all trials.

in units of $\mathrm{Km^2s^{-1}}$. Note, that raw data for both heat fluxes and ROS values have extremely large associated uncertainties. Observed ROS values vary by nearly a factor of two, depending on the measurement technique used. While we have included only locations with ignition confirmed by video footage in our calculations, heat fluxes still vary up to a factor of four between sensors.

For comparison, we also obtain an LES-based integrated fireline intensity value I_{LES}. Due to wind shear, as measured by the sounding launched prior to the burn (10:00:00 CST), the CWI direction at the surface differs from the one used to estimate CWI smoke. I_{LES} was, hence, estimated by assuming 125 degree rotation of LES fields, based on the lowest available wind direction measurement. We use trapezoidal rule to numerically integrate the mean crosswind heat flux along the depth of the fireline (see Appendix D) and find $I_{LES} = 1002\ \mathrm{Km^2s^{-1}}$.

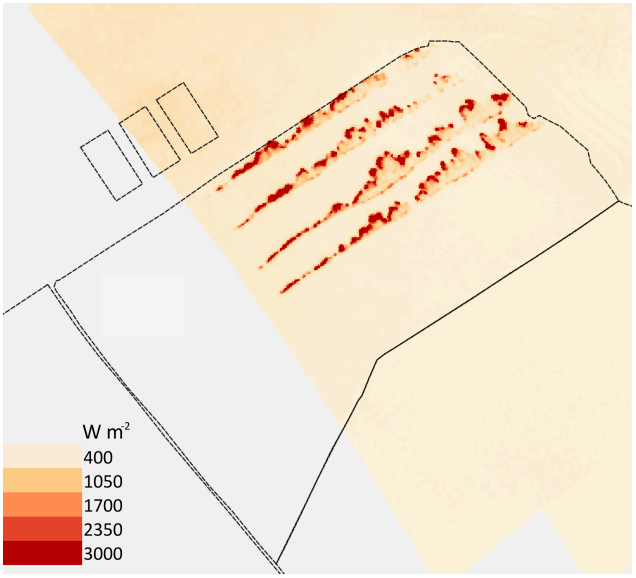

Figure 8. Long wave infra-red (LWIR) image of L2G lot during ignition (12:32:02 CST) with dashed black lines denoting burn perimeters.

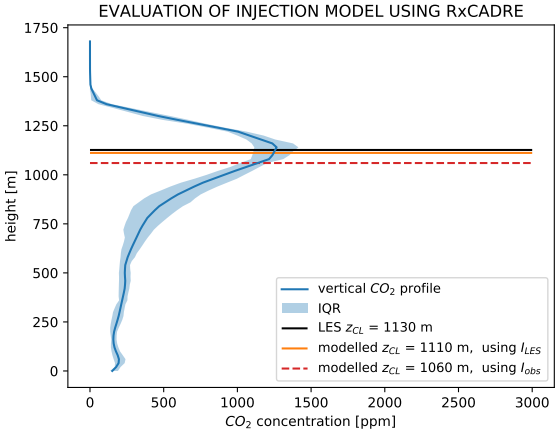

Figure 9. Model evaluation using a case-study of a real prescribed burn (RxCADRE 2012). CWI smoke concentration profile shown in blue. "True" z_{CL} obtained directly from LES shown in solid black. Solid orange and dashed red lines correspond to z_{CL} estimates obtained using the iterative solution of the proposed smoke injection height parameterization (Eq. (8)), based on LES- and observations- derived fireline intensities, respectively.

We apply our iterative solution (Eq. (8)) to find two z_{CL} estimates based on I_{obs} and I_{LES}, and compare them to the CWI smoke injection height obtained from the LES. The results are shown in Fig. 9. The parameterized injection heights are under-predicted by 20 m and 70 m for LES- and observations- derived I values, respectively.

5 Discussion

5.1 Plume Classification

In previous sections we apply an energy balance parameterization to predict the mean smoke injection height z_{CL} of a given penetrative plume. For this purpose, only plumes rising above ABL top z_i were included in the synthetic plume dataset used to constrain and evaluate the approach (see Table B1). In this section, we step back and consider all performed simulations, to determine whether the same equations can also be used to classify penetrative vs. non-penetrative plumes.

The synthetic dataset described in 2.2 consisted of 140 runs and excluded 7 simulations, where the plume remained trapped in the ABL (see Table B1 and Table 3). We determined this by visual analysis of CWI centerline and smoke fields. The excluded plumes typically exhibited oscillatory or irregular centerline behavior (within the ABL, such as shown in the example in Fig. B1) with little or no smoke injected above z_i. For several combinations of fire and atmospheric conditions, however, making the distinction was challenging. For this reason, we included these "marginally-penetrative" plumes in the dataset.

In real-world applications, classification is a fundamental first step in plume rise parameterization process Sofiev et al. (2012) . A viable automated method for categorizing penetrative vs. non-penetrative plumes requires that the distinction be made based on available input parameters, rather then smoke observations (as such are typically not available at the time of making a forecast).

Conveniently, we can use Eq. (8) to obtain a z_{CL} estimate for any combination of input parameters without prior knowledge of plume type. It can, hence, be applied as a classifier by requiring that for a penetrative plume

$$z_{CL} > z_{i+} \tag{11}$$

where z_{i+} denotes the height of the upper edge of the numerical grid box (or ambient atmospheric sounding) containing z_i. In other words, this definition ensures that z_i and z_{CL} are not in the same vertical model level. If this condition is not satisfied, the plume is assumed to be non-penetrative.

This approach correctly classifies all non-penetrative plumes that had been identified by visual analysis (Table 3). In addition, several plumes exhibiting marginal behavior are also classified by Eq. (11) to be non-penetrative.

For the purpose of subsequent dispersion modelling within real-world applications, non-penetrative plumes (i.e. all plumes listed in Table 3) would be assumed to become uniformly mixed in the vertical within a few convective turnover distanced downwind of the fire. Turbulent eddies within the ABL produce a well-mixed layer, resulting in relatively homogeneous vertical distribution of pollutants between the surface and z_i. In contrast, for plumes that extend above z_i, spanning the ABL, the entrainment layer, and/or the free troposphere, subsequent dispersion is typically handled by trajectory models.

5.2 Comparison with Existing Models

The above model evaluation indicates encouraging performance for the proposed smoke injection parameterization (Eq. (8)) at little computational cost. An additional advantage of our method is that it does not require making simplifying assumptions

Table 3. Identifying non-penetrative plumes using visual analysis vs. automated classification. Plume name denotes wind condition **W**, fuel type **F** and initial atmospheric profile **R**.

Plume	Visual analysis	Automated classification
W5F9R1	✓	✓
W5F1R3	✓	✓
W5F8R3	✓	✓
W5F9R3	✓	✓
W5F1R7	✓	✓
W5F8R7	✓	✓
W5F9R7	✓	✓
W5F1R0		✓
W5F1R1		✓
W5F8R1		✓
W5F10R3		✓
W5F11R3		✓
W5F1R4		✓
W5F11R4		✓

regarding the shape and heat flux distribution of the fire. This allows us to easily apply our model to complex heat sources, such as one produced with the strip head fire ignition pattern during the RxCADRE L2G prescribed burn (Fig. 8).

Unlike most existing plume rise parameterizations (Briggs, 1975; Rio et al., 2010; Freitas et al., 2007) we focus on a CWI centerline. Our model can be viewed as a "bulk method", having some common ground with the thermodynamic approach used in the FireWork modelling framework (Anderson et al., 2011; Chen et al., 2019) and the energy balance approach proposed by Sofiev et al. (2012). More specifically, we make no attempt to predict the full evolution of the rising plume centerline velocity or temperature before it reaches its equilibrium height. Rather, we focus on the energy balance of the plume over a "penetration layer".

Through analysis of the 140 LES experiments for plumes under variable fire and atmospheric conditions, we found that near-surface and boundary-layer plume dynamics are extraordinarily complex. While some aspects of plume mixing can be reasonably accounted for by making traditional entrainment assumptions, complicated features resulting from fire-atmosphere coupling, such as formation of lateral vortices and fireline wind convergence zone, are difficult to parameterize directly. Hence, we apply the energy balance approach to a layer well above the surface, starting from a reference height z_s close to the top of the ABL.

As noted in Sect. 3, the implicit functional form of our solution (Eq. (8)) can be interpreted as a characteristic timescale multiplied by the characteristic velocity scale w_f. By rearranging Eq. (7) and substituting Eq. (8) for z' it can be shown that

the two expressions for w_f are equivalent, namely:

$$w_f = \left[\frac{I}{z_i \theta'}\right] = \left[\frac{g I z'}{\theta_s z_i}\right]^{\frac{1}{3}} \tag{12}$$

The scaling relationship between vertical plume velocity and cubic root of fire heat has been previously established with both Rio's and Freita's models (Rio et al., 2010; Freitas et al., 2007), although our formulation includes different variables inside the radical. While both of our forms for w_f and both model formulations (the simplified Eq. (7) and the expanded Eq. (8)) are mathematically equivalent, conversion from one form to another requires raising terms to 6$^{\text{th}}$ power. This results in large prediction errors; hence, for practical applications, the full Eq. (8) should be used.

5.3 Dimensionless Relationship

As discussed in Sect. 3, we can obtain an explicit solution for z_{CL} by making additional assumptions about the vertical profile of potential temperature above the ABL. This allows us to reduce our Eq. (9) to a similarity relationship with two dimensionless groups $\overline{z}$ and $\overline{H}$, denoting the left hand side (LHS) and right hand side (RHS) of Eq. (13), respectively. Nondimensional $\overline{z}$ and $\overline{H}$ are linearly related, as shown in Fig. 10. The simple relationship suggests that our modelling results could fairly easily be scaled to a wider range of fire and atmospheric conditions, beyond those captured by the synthetic dataset presented in the paper.

$$\underbrace{\frac{z'}{z_i}}_{\overline{z}} = \underbrace{C^{\frac{3}{2}} \left[\frac{\theta_s}{g\gamma^3}\right]^{\frac{1}{4}} \left[\frac{I}{z_i^3}\right]^{\frac{1}{2}}}_{\overline{H}} \tag{13}$$

5.4 Model Bias

The raw, non-bias- corrected form of the model suffers from a positive bias for tall plumes, as suggested by Fig. 5c and 6c. In other words, z_{CL} is overpredicted for plumes injected high above the ABL. We speculate that this is due to the simplifying assumption that most of the cooling, mixing, and dilution occurs below the reference level z_s in upper portion of the ABL.

As the distance between z_s and z_{CL} increases for tall plumes and as the smoke travels further into the free atmosphere, this assumption becomes increasingly less accurate. Additional radiative cooling and entrainment of ambient air is, therefore, unaccounted for, resulting in over-prediction for z_{CL}.

This issue is largely resolved for our dataset with the applied bias-correction. However, cases with strong shear turbulence and active smoke mixing above the ABL are still likely to be overestimated.

5.5 Limitations

The most significant limitation of the proposed smoke injection height parameterization is that it applies only to smoke plumes with no water vapor condensation. Latent heat effects are not considered. Hence, smoke injection level for extreme pyroconvective events (e.g. flammagenitus clouds (WMO, 2017)) will likely be grossly under-predicted with the given formulation.

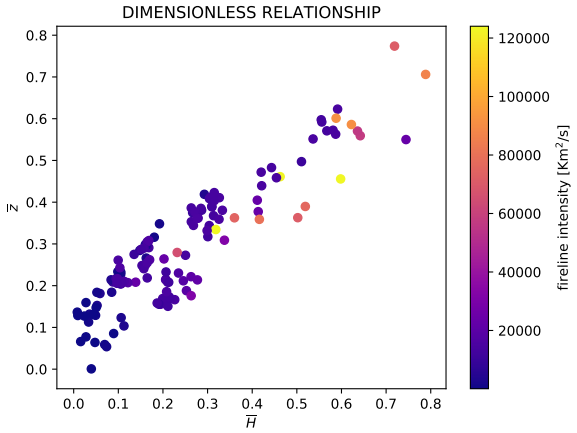

Figure 10. Similarity solution for dimensionless groups $\overline{H}$ and $\overline{z}$, corresponding to the RHS and LHS of Eq. (13), respectively. Scatter points represent individual LES runs, colored by fireline intensity parameter I.

Therefore, in its current form, our parameterization is unlikely to be suitable for large-scale applications (e.g. global chemical transport models). However, it has the potential to improve regional air quality tools (e.g. BlueSky), since wildfire emissions sources are largely dominated by in- or near- ABL non-condensing smoke plumes (Val Martin et al., 2010, 2018).

Given the energy-balance formulation of our plume rise parameterization, it may be possible to incorporate latent heat effects by including an extra PE term in Eq. (1). Similarly to the iterative process for finding a level of neutral buoyancy with Eq. (8) using potential temperature, it may be possible to predict plume condensation level using ambient humidity profile. However, a big obstacle to this development is that, to our knowledge, WRF-SFIRE has not been validated for such conditions.

Unlike many existing methods, our parameterization relies on fireline intensity parameter I, rather than average fire heat flux values, as input. While this approach offers an advantage for modelling plumes from complex ignition sources (such as shown in Fig. 8), fireline intensity is difficult to observe in the field.

Another limitation is the inherently implicit form of the full model Eq. (8). While we have not encountered any issues using an iterative solver to find z_{CL}, atypical (or extremely noisy) ambient atmospheric soundings could potentially affect convergence. The explicit form (Eq. (9)) derived using the idealizing ambient sounding (Fig. 4) offers a possible solution for such cases. However, it fails for weakly stable and adiabatic free atmosphere (eg. condition R8 in Fig. 1), as θ_s is extrapolated into lower levels of ABL.

Lastly, the model has been developed and tested only for typical daytime atmospheric conditions. We have not assessed model performance for stable night-time atmospheric profiles or in the presence of strong vertical windshear.

6 Conclusions

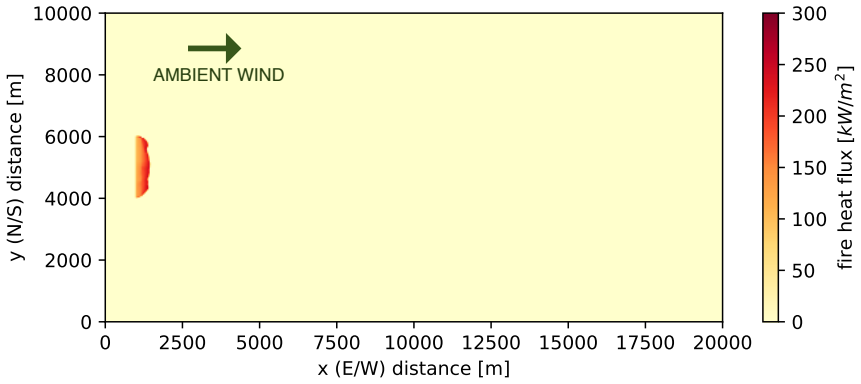

Figure A1. Numerical domain setup.

Plume rise estimation remains one a weak link in our ability to forecast where and how smoke from wildfires travels in the atmosphere. In this study we present a simple parameterization (Eq. (8)) for predicting CWI smoke-plume centerline height from a wildfire of an arbitrary shape and intensity. Our approach is based on energy-balance of the plume over a penetration region. We constrain and evaluate the proposed ~~model,~~ method using a synthetic LES-derived plume dataset developed for a wide range of fire and atmospheric conditions.

Based on the results of cross-evaluation with LES data as well as a real prescribed burn case study, the parameterization offers reasonable accuracy at little computational cost. We ~~hope that the proposed approach~~ demonstrate that the approach can also be applied as a classifier to distinguish penetrative and non-penetrative plumes. This information is key for subsequent dispersion modelling, as plume behavior is governed by different physics above and below the ABL. The proposed method can be used as a sand-alone deterministic model or embedded in a host smoke modelling framework.

We hope that parameterization presented in this study will be of interest to air-quality researchers to provide a low-cost solution for regional wildfire emissions-modelling applications.

Code availability. S1: WRF-SFIRE sample initialization files (sample_simulation.zip)

Appendix A: Domain Setup

Appendix B: Parameter space of LES dataset

Table B1 and Table B2 summarize the tested combinations of fire and atmospheric parameters captured by the synthetic plume dataset. Colored cells correspond to completed simulations. Tall boundary layers of **R5** and **R6** domains required low winds (5 ms^{-1} and below) and high intensity fires (fuel categories 4, 6, 7, 12 and 13) to reach ABL top within the simulation

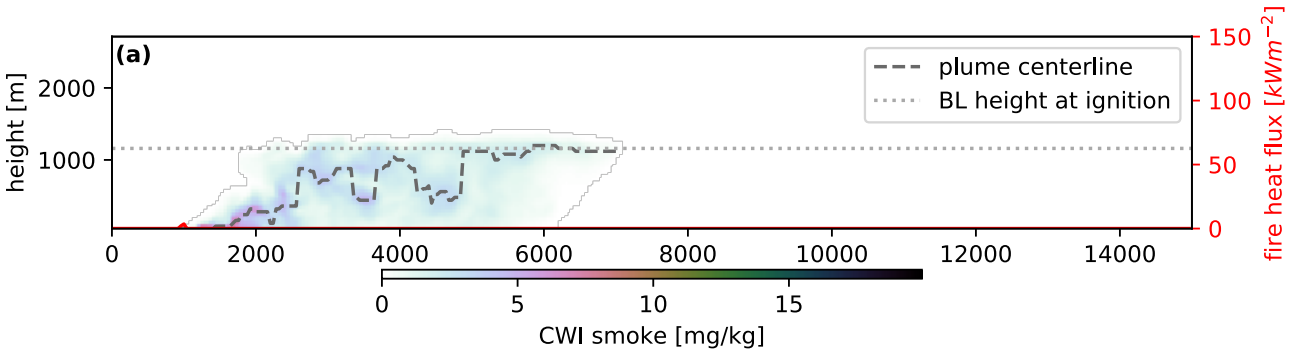

Figure B1. Fixed aspect ratio plot of CWI smoke from a sample non-penetrative plume (W5F8R3). Plume centerline and z_i shown in dashed and dotted grey, respectively.

runtime and/or avoid smoke recirculation. Hence, alternative combinations (white cells in **R5** and **R6** columns) would require considerably different domain setup from other runs. For this reason these combinations were not tested. Also, a single run was performed for **R8** condition (adiabatic free atmosphere) as an extreme case scenario.

Red cells in Tab. B2 highlight simulations that were completed, but subsequently excluded from analysis presented in Sect. 3. This was done based on visual inspection of LES fields. There were two possible reasons for exclusion: (i) the plume reached the top of the domain or (ii) the plume appeared to be non-penetrative. In the former case, it's questionable whether the fields are physical, as the plume could potentially be affected by the absorbing layer near domain top, designed to prevent numerical instability. The latter rendered the plume irrelevant for the purpose of analysis presented in Sect. 3. These non-penetrative runs, however, were included for testing the plume classification method presented in Sect. 5.1.

Appendix C: Identifying Quasi-Stationarity

We define the quasi-stationary downwind region for each plume based on two factors: the height of the centerline and tracer concentration gradient along the centerline. Our filter attempts to extract only those portions of the downwind CWI smoke distribution, where both of these factors are changing slowly.

First, we remove the effect of random turbulent oscillations by applying a smoothing function (Savitzky-Golay filter provided by SciPy library with polynomial order set to 3) to both the concentration gradient along the centerline and the centerline height. We vary the size of the smoothing window as a function of mean ambient wind condition **W**, such that $window\_length = max(\mathbf{W} \cdot 10 + 1, 51)$ grid points.

The filter then applies the following criteria to extract quasi-stationary regions:

- smoothed tracer concentration along the plume centerline varies by less then 10% of the maximum concentration gradient
- smoothed centerline height varies by less then a 100 m

Table B1. Combinations of test conditions resulting in penetrative plumes, as captured by the LES datasets. Green cell highlights fireline length condition (**L**) runs. Intensity of blue color corresponds to the number of runs for fuel condition (**F**) represented by the cell. Row 'W5' is expanded in Table B2 below.

R/W	R0	R1	R2	R3	R4	R5*†	R6*†	R7*	R8*
W3	F7	F7	F7	F7	F7	F7	F7	F7	
W4	F7	F7	F7	F7	F7L1 F7L2 F7L4	F7	F7	F7	
W5	F1 - F12, excl:F4	F1 - F13, excl:F9	F1 - F13	F2 - F13, excl:F8,F9	F1 - F13	F4 F6 F7 F12 F13	F4 F6 F7 F12 F13	F2 - F13, excl:F8,F9	F7
W6	F7	F7	F7	F7	F7			F7	
W7	F7	F7	F7	F7	F7			F7	
W8	F7	F7	F7	F7	F7			F7	
W9	F7	F7	F7	F7	F7			F7	
W10	F7	F7	F7	F7	F7			F7	
W11	F7	F7	F7	F7	F7			F7	
W12	F7	F7	F7	F7	F7			F7	

*Deep domain (5 km). †Extended runtime (30 min).

Table B2. Tested combinations of fuel and ABL conditions (all blue and red colored cells).

R/W	R0	R1	R2	R3	R4	R5*†	R6*†	R7*	R8*
F1				ABL plume				ABL plume	
F2									
F3									
F4	smoke at domain top								
F5									
F6									
F7									
F8				ABL plume				ABL plume	
F9		ABL plume		ABL plume				ABL plume	
F10									
F11									
F12									
F13	smoke at domain top								

*Deep domain (5 km). †Extended runtime (30 min).

- the location is downwind of the maximum tracer concentration gradient
- the location is at least 10 grid points away from the maximum in smoothed and non-smoothed centerline height
- the location is at least 50 grid points away from the downwind endpoint of the centerline

The above thresholds were determined through an informal sensitivity analysis (not shown), based on the filter's ability to effectively identify regions of near-stationary plume centerline height for all simulations in our dataset.

Appendix D: Estimating Model Input Parameters

Summarized in Table D1 are parameters associated with an iterative solution for z_{CL} using Eq. (8). Below is our approach to estimating these parameters from LES data.

As noted above, we consider the problem in crosswind direction. Given a three-dimensional fire of an arbitrary shape (eg. Fig. 2b) and an ambient atmospheric sounding, we first average the fire kinematic heat flux for all ignited cells (where heat flux > 1 $\mathrm{kWm^{-2}}$) over the crosswind (y) direction at the surface (red line on Fig. 2a). Due to surface wind shear this direction

Table D1. Variable descriptions and units used in smoke injection model.

Variable	Unit	Description
I	$\mathrm{Km^2s^{-1}}$	fireline integrated heat flux
g	$\mathrm{ms^{-2}}$	gravity constant = 9.81
θ_{CL}	K	ambient potential temperature at z_{CL}
θ_s	K	ambient potential temperature at z_s
z_{CL}	m	smoke injection height
z_i	m	boundary layer height
z_s	m	reference height

may differ from the one used for calculating CWI smoke concentrations (as shown in Sect. 4.3). To obtain fireline intensity parameter I we numerically integrate the crosswind averaged heat fluxes over the depth of the fireline in the along-wind (x) direction.

We use pre-ignition potential temperature profile (i.e. the ambient environment upwind of the fire) averaged over the entire LES domain as an environmental sounding. All model fields are interpolated to have a 20 m vertical increment. z_i is defined as the height of the strongest environmental lapse rate gradient, and $z_s = \frac{3}{4} z_i$, based on informal model sensitivity analysis (not shown). The exact choice of z_s has little effect on model performance as long as it remains within the upper portion of the uniform potential temperature well-mixed layer.

The values of θ_s and θ_{CL} are then determined from the pre-ignition sounding for each simulation using the definitions of z_s and z_{CL} (as described in Sect. 2.3).

Appendix E: Iterative Solution for z_{CL}

The numerical implementation of our iterative solution using SciPy's fsolve function (scipy.optimize.fsolve) is as follows. We rewrite bias corrected Eq. (8) into an input function $toSolve$ as:

$$toSolve = lambda\ z : z - B_1(z_s + C\left[\frac{g(T0[int(\frac{z}{dz})] - \theta_s)}{\theta_s(z - z_s)}\right]^{-\frac{1}{2}}\left[\frac{gI(z - z_s)}{\theta_s z_i}\right]^{\frac{1}{3}}) - B_2 \tag{E1}$$

where $C = 1.005$, $B_1 = 0.924$ and $B_2 = 116.417$ are bias correction parameters, $T0$ is the potential temperature sounding vector, dz is the vertical step and $int()$ is a standard Python function converting the bracketed value into an integer.

A possible issue for some solvers is that we are, effectively, iterating over the vertical index of the column vector $T0$ corresponding to z_{CL}. As the numerical solver attempts to converge on a solution it may query a non-existent index and fail. We are able to obtain a fast and consistent performance by ensuring we set z_i as the initial guess for z_{CL} and by minimizing the initial step bound option of the solver

$$z_{CL} = fsolve(toSolve, z_i, factor = 0.1) \tag{E2}$$

Author contributions. Conceptualization: Nadya Moisseeva and Roland Stull; methodology: Nadya Moisseeva; resources: Roland Stull; data curation: Nadya Moisseeva; writing (original draft preparation): Nadya Moisseeva and Roland Stull; writing (review and editing): Nadya Moisseeva and Roland Stull; visualization: Nadya Moisseeva; supervision: Roland Stull; funding acquisition: Nadya Moisseeva and Roland Stull

Competing interests. The authors declare that they have no conflict of interest.

Acknowledgements. We sincerely thank Dr. Rosie Howard and Chis Rodell for the countless fruitful discussions, new ideas and encouragement. We would like to acknowledge WestGrid and ComputeCanada for providing computational resources for LES runs, and Julia Jeworrek for her ongoing generous help with cluster access. Thank you to all members of UBC Weather Research and Forecasting Team for their motivation and support. This work was funded by grants from Natural Sciences and Engineering Research Council of Canada (NSERC), Natural Resources Canada (NRCan), Fraser Basin Council (BC CLEAR), British Columbia Ministry of Environment and Climate Change Strategy, Alberta Ministry of Environment and Parks and Government of the Northwest Territories.

References

Anderson, H. E.: Aids to determining fuel models for estimating fire behavior, The Bark Beetles, Fuels, and Fire Bibliography, p. 143, 1982.

Anderson, K., Pankratz, A., and Mooney, C.: 9.2 A thermodynamic approach to estimating smoke plume heights, in: Proceedings of Ninth Symposium on Fire and Forest Meteorology, Palms Springs, CA, pp. 17–21, 2011.

Briggs, G.: Plume Rise Equations, pp. 59–111, AMS: Boston, MA, USA, 1975.

Butler, B., Teske, C., Jimenez, D., O'Brien, J., Sopko, P., Wold, C., Vosburgh, M., Hornsby, B., and Loudermilk, E.: Observations of energy transport and rate of spreads from low-intensity fires in longleaf pine habitat –RxCADRE 2012, International Journal of Wildland Fire, 25, 76–89, http://dx.doi.org/10.1071/WF14154, 2016.

Chen, J., Anderson, K., Pavlovic, R., Moran, M. D., Englefield, P., Thompson, D. K., Munoz-Alpizar, R., and Landry, H.: The FireWork v2.0 air quality forecast system with biomass burning emissions from the Canadian Forest Fire Emissions Prediction System v2.03, Geoscientific Model Development, 12, 3283–3310, https://doi.org/10.5194/gmd-12-3283-2019, https://www.geosci-model-dev.net/12/3283/2019/, 2019.

Clements, C. B., Potter, B. E., and Zhong, S.: In situ measurements of water vapor, heat, and CO2 fluxes within a prescribed grass fire, International Journal of Wildland Fire, 15, 299–306, 2006.

Coen, J. L., Cameron, M., Michalakes, J., Patton, E. G., Riggan, P. J., and Yedinak, K. M.: WRF-Fire: Coupled Weather–Wildland Fire Modeling with the Weather Research and Forecasting Model, Journal of Applied Meteorology and Climatology, 52, 16–38, https://doi.org/10.1175/JAMC-D-12-023.1, http://dx.doi.org/10.1175/JAMC-D-12-023.1, 2012a.

Coen, J. L., Cameron, M., Michalakes, J., Patton, E. G., Riggan, P. J., and Yedinak, K. M.: WRF-Fire: Coupled Weather–Wildland Fire Modeling with the Weather Research and Forecasting Model, Journal of Applied Meteorology and Climatology, 52, 16–38, https://doi.org/10.1175/JAMC-D-12-023.1, http://dx.doi.org/10.1175/JAMC-D-12-023.1, 2012b.

Cushman-Roisin, B.: Atmospheric boundary layer, Environmental Fluid Mechanics, pp. 165–186, 2014.

Freitas, S. R., Carvalho, J., Longo, K., Chatfield, R., Latham, D., Silva Dias, M., Andreae, M., Prins, E., Santos, J., and Gielow, R.: Including the sub-grid scale plume rise of vegetation fires in low resolution atmospheric transport models, Atmospheric Chemistry and Physics, pp. 3385–3398, 2007.

Goodrick, S. L., Achtemeier, G. L., Larkin, N. K., Liu, Y., and Strand, T. M.: Modelling smoke transport from wildland fires: a review, International Journal of Wildland Fire, 22, 83–94, 2013.

Heilman, W. E., Liu, Y., Urbanski, S., Kovalev, V., and Mickler, R.: Wildland fire emissions, carbon, and climate: Plume rise, atmospheric transport, and chemistry processes, Forest Ecology and Management, 317, 70–79, 2014.

Ichoku, C., Kahn, R., and Chin, M.: Satellite contributions to the quantitative characterization of biomass burning for climate modeling, Atmospheric Research, 111, 1 – 28, https://doi.org/https://doi.org/10.1016/j.atmosres.2012.03.007, http://www.sciencedirect.com/science/article/pii/S0169809512000750, 2012.

Jimenez, D. and Butler, B.: RxCADRE 2012: RxCADRE 2012: In-situ fire behavior measurements, https://doi.org/https://doi.org/10.2737/RDS-2016-0038, 2016.

Kochanski, A. K., Jenkins, M. A., Mandel, J., Beezley, J. D., Clements, C. B., and Krueger, S.: Evaluation of WRF-SFIRE performance with field observations from the FireFlux experiment, Geosci. Model Dev., 6, 1109–1126, https://doi.org/10.5194/gmd-6-1109-2013, http://www.geosci-model-dev.net/6/1109/2013/, 2013.

Kochanski, A. K., Mallia, D. V., Fearon, M. G., Mandel, J., Souri, A. H., and Brown, T.: Modeling Wildfire Smoke Feedback Mechanisms Using a Coupled Fire-Atmosphere Model With a Radiatively Active Aerosol Scheme, Journal of Geophysical Research: Atmospheres, 124, 9099–9116, 2019.

Larkin, N. K., O'Neill, S. M., Solomon, R., Raffuse, S., Strand, T., Sullivan, D. C., Krull, C., Rorig, M., Peterson, J., and Ferguson, S. A.: The BlueSky smoke modeling framework, International Journal of Wildland Fire, 18, 906–920, 2010.

Mallia, D. V., Kochanski, A. K., Urbanski, S. P., and Lin, J. C.: Optimizing smoke and plume rise modeling approaches at local scales, Atmosphere, 9, 166, 2018.

Mallia, D. V., Kochanski, A. K., Urbanski, S. P., Mandel, J., Farguell, A., and Krueger, S. K.: Incorporating a Canopy Parameterization within a Coupled Fire-Atmosphere Model to Improve a Smoke Simulation for a Prescribed Burn, Atmosphere, 11, 832, 2020.

Mandel, J., Amram, S., Beezley, J., Kelman, G., Kochanski, A., Kondratenko, V., Lynn, B., Regev, B., and Vejmelka, M.: Recent advances and applications of WRF–SFIRE, Natural Hazards and Earth System Sciences, 14, 2829–2845, 2014.

Moisseeva, N. and Stull, R.: Capturing Plume Rise and Dispersion with a Coupled Large-Eddy Simulation: Case Study of a Prescribed Burn, Atmosphere, 10, 579, 2019.

Ottmar, R. D., Hiers, J. K., Butler, B. W., Clements, C. B., Dickinson, M. B., Hudak, A. T., O'Brien, J. J., Potter, B. E., Rowell, E. M., Strand, T. M., and Zajkowski, T. J.: Measurements, datasets and preliminary results from the RxCADRE project –2008, 2011 and 2012, International Journal of Wildland Fire, 25, 1–9, http://dx.doi.org/10.1071/WF14161, 2016.

Paugam, R., Wooster, M., Freitas, S., and Val Martin, M.: A review of approaches to estimate wildfire plume injection height within large-scale atmospheric chemical transport models, Atmospheric Chemistry and Physics, 16, 907–925, https://doi.org/10.5194/acp-16-907-2016, https://www.atmos-chem-phys.net/16/907/2016/, 2016.

Pavlovic, R., Chen, J., Anderson, K., Moran, M. D., Beaulieu, P.-A., Davignon, D., and Cousineau, S.: The FireWork air quality forecast system with near-real-time biomass burning emissions: Recent developments and evaluation of performance for the 2015 North American wildfire season, Journal of the Air & Waste Management Association, 66, 819–841, 2016.

Prichard, S., O'Neill, S., and Urbanski, S.: Evaluation of revised emissions factors for emissions prediction and smoke management, https://www.epa.gov/sites/production/files/2017-10/documents/prichard.pdf, 2017.

Prichard, S., Larkin, N. S., Ottmar, R., French, N. H., Baker, K., Brown, T., Clements, C., Dickinson, M., Hudak, A., Kochanski, A., et al.: The Fire and Smoke Model Evaluation Experiment—A Plan for Integrated, Large Fire–Atmosphere Field Campaigns, Atmosphere, 10, 66, 2019.

Raffuse, S. M., Craig, K. J., Larkin, N. K., Strand, T. T., Sullivan, D. C., Wheeler, N. J., and Solomon, R.: An evaluation of modeled plume injection height with satellite-derived observed plume height, Atmosphere, 3, 103–123, 2012.

Rio, C., Hourdin, F., and Chédin, A.: Numerical simulation of tropospheric injection of biomass burning products by pyro-thermal plumes, Atmospheric Chemistry and Physics, 10, https://doi.org/10.5194/acp-10-3463-2010, 2010.

Sofiev, M., Ermakova, T., and Vankevich, R.: Evaluation of the smoke-injection height from wild-land fires using remote-sensing data, Atmospheric Chemistry and Physics, 12, 1995–2006, https://doi.org/10.5194/acp-12-1995-2012, https://www.atmos-chem-phys.net/12/1995/2012/, 2012.

Val Martin, M., Logan, J. A., Kahn, R. A., Leung, F.-Y., Nelson, D. L., and Diner, D. J.: Smoke injection heights from fires in North America: analysis of 5 years of satellite observations, Atmospheric Chemistry and Physics, 10, 1491–1510, https://doi.org/10.5194/acp-10-1491-2010, https://www.atmos-chem-phys.net/10/1491/2010/, 2010.

Val Martin, M., Kahn, R. A., Logan, J. A., Paugam, R., Wooster, M., and Ichoku, C.: Space-based observational constraints for 1-D fire smoke plume-rise models, Journal of Geophysical Research: Atmospheres, 117, 2012.

Val Martin, M., Kahn, R., and Tosca, M.: A Global Analysis of Wildfire Smoke Injection Heights Derived from Space-Based Multi-Angle Imaging, Remote Sensing, 10, 1609, 2018.

WMO, W. M. O.: International Cloud Atlas, World Meteorological Organization, https://cloudatlas.wmo.int/en/flammagenitus.html, 2017.